

Aus dem Walther-Straub-Institut für Pharmakologie
und Toxikologie

Institut der Universität München

Vorstand: Prof. Dr. med. Thomas Gudermann



Optimization of a mitochondrial calcium uptake enhancer for the treatment of cardiac arrhythmia

Dissertation

zum Erwerb des Doktorgrades der Medizin

an der Medizinischen Fakultät

der Ludwig-Maximilians-Universität zu München

vorgelegt von

Anna Sophia Schedel

aus

Würzburg

Jahr 2023

i.

Mit Genehmigung der Medizinischen Fakultät
der Universität München

Berichterstatter: Prof. Dr. med. Thomas Gudermann

Mitberichterstatter: Prof. Dr. Stefan Kääb

Prof. Dr. Christopher Reithmann

Mitbetreuung durch den
promovierten Mitarbeiter:

PhD Johann Schredelseker

Dekan: Prof. Dr. med. Thomas Gudermann

Tag der mündlichen Prüfung: 21.12.2023

Contents

1	Abstract	1
2	Introduction	2
2.1	Cardiovascular diseases	2
2.2	Electrophysiological principles of the heart and the origin of cardiac arrhythmia 3	
2.2.1	Functional organization of the heart muscle	3
2.2.2	Cardiac excitation-contraction coupling and intracellular calcium (Ca ²⁺) signaling	3
2.2.3	Pathophysiology of arrhythmia and its pharmacological therapy	5
2.3	Ca ²⁺ signaling in cardiovascular diseases	7
2.4	Mitochondrial Ca ²⁺ uptake as therapeutic approach in arrhythmia	7
2.4.1	Voltage dependent anion channel (VDAC) in mitochondrial Ca ²⁺ transfer and antiarrhythmic treatment	9
2.4.2	Efsevin as promising mitochondrial Ca ²⁺ uptake enhancer (MiCUp) in the treatment of cardiac arrhythmia	9
2.5	Aim and objectives	10
3	Material and Methods	12
3.1	Efsevin and its analogs	12
3.2	Molecular docking	14
3.2.1	Docking process	14
3.2.2	Docking analysis/evaluation/ranking	14
3.3	Zebrafish experiments	15
3.3.1	Zebrafish phenotype rescue experiment	15
3.4	HL-1 cells	16
3.4.1	HL-1 cardiomyocyte culture	16
3.4.2	Mitochondrial Ca ²⁺ uptake measurements	18
3.5	Evaluation methods	20
3.5.1	Statistical analysis	20
3.5.2	Graphical presentation	20
4	Results	21
4.1	Screening of efsevin derivatives using computational docking	21
4.2	<i>In vivo</i> screening of derivatives performing phenotype rescue experiment in zebrafish embryos	22
4.3	Quantification of SR-mitochondria Ca ²⁺ transfer in HL-1 cardiomyocytes ...	25
5	Discussion	28
5.1	Summary	28

5.2	Limitations of applied screening methods and potential follow-up studies....	28
5.3	Further possible studies on MiCUp candidates.....	29
5.4	Probable causes and evaluation of obtained outcomes	30
6	Abbreviations	32
7	List of Figures	34
8	References	35
9	Acknowledgement.....	40
10	Affidavit	41

1 Abstract

Efsevin was previously shown to be a potential suppressor of cardiac arrhythmogenesis by enhancing mitochondrial Ca^{2+} uptake. VDAC2, located in the OMM, was identified as primary target of efsevin mediating the Ca^{2+} -transfer into mitochondria¹. However, previous data of SR-mitochondria Ca^{2+} transfer in HL-1 cells have demonstrated a relatively high half-maximal activity (of $4.4\mu\text{M}$) which determines its clinical usage and potency due to high dosing to obtain an overall effect in humans as well as posing applicational problems in terms of drug amounts. In addition, efsevin has limited stability due to early hydrolyzation as demonstrated in liver microsomes².

Therefore, in this study, I aimed to evaluate chemically modified efsevin derivatives in order to optimize its pharmacodynamics, describing the first study providing a comprehensive pharmacological potency and efficacy analysis of forty efsevin derivatives as potential mitochondrial Ca^{2+} uptake enhancers (MiCUp).

In silico molecular docking screening revealed no improvement in binding affinities of any derivative. However, slightly improved dose-dependent effects of three tested derivatives (P105D03, P105E03 and P105B10) were present in the *in vitro* experiments, demonstrating a small increase in EC50 values when directly compared to efsevin indicating improved affinity. Moreover, compound P105D03 showed an increase in embryonic zebrafish heartbeat restoration in the *in vivo* experiments.

In summary, when we combine the results of the three screening methods, no clear superiority of a particular type of chemical modification could be observed indicating a specific chemical optimization of efsevin as MiCUp. However, based on the finding that chemical modifications display measurable differences in derivatives' potency in two out of three screening methods, this approach seems to affect mitochondrial Ca^{2+} uptake. Therefore, chemical modification of potential MiCUps remain a valuable target for future research.

Zusammenfassung (german):

Die Substanz Efsevin hat sich kürzlich als potenzielles Therapeutikum von Herzrhythmusstörungen durch Verbesserung der mitochondrialen Kalizumaufnahme erwiesen. Der spannungsabhängige Anionen-Kanal 2 (VDAC2), welcher den Kalziumtransfer in die Mitochondrien vermittelt und in der äußeren Mitochondrienmembran lokalisiert ist, konnte als primäres Ziel von Efsevin identifiziert werden¹. Generierte Daten zum Kalziumtransfer zwischen Sarkoplasmatischem Retikulum und Mitochondrium in Kardiomyozyten der Zelllinie HL-1 stellten jedoch eine relativ hohe halbmaximale Aktivität (von $4,4\mu\text{M}$) der Substanz Efsevin fest². Hierdurch ist die klinische Anwendung im menschlichen Organismus aufgrund der hohen erforderlichen Dosierung zum Erreichen einer Gesamtwirkung eingeschränkt und wirft Anwendungsprobleme in Bezug auf die Medikamentendosierung auf.

Darüber hinaus wurde in Lebermikrosomen eine geringe Stabilität von Efsevin aufgrund früher Hydrolyse nachgewiesen.

Erstmals wurden in dieser Arbeit, anhand von umfassender pharmakologischer Potenz- und Wirksamkeitsanalysen, chemisch modifizierte Efsevin-Derivate mit dem Ziel einer Optimierung der mitochondrialen Kalziumaufnahme untersucht.

Das *in-silico*-Experiment mittels molekularen Dockings ergab keine Verbesserung der Bindungsaffinität eines bestimmten Derivats.

Drei der untersuchten Derivate (P105D03, P105E03 und P105B10) wiesen jedoch im direkten Vergleich mit Efsevin leicht verbesserte dosisabhängige Wirkungen im *in-vitro*-Experiment auf und verzeichneten einen Anstieg des EC₅₀-Werts als Hinweis auf eine optimierte Affinität. Darüber hinaus zeigte die Substanz P105D03 eine Zunahme der Herzschlagwiederherstellung bei embryonalen Zebrafischen im *in-vivo*-Experiment.

Zusammenfassend betrachtet ließ sich bei der Ergebnisanalyse der drei Untersuchungsmethoden keine klare Überlegenheit eines Efsevin-Derivats feststellen, wodurch auf keine Wirksamkeitssteigerung einer getesteten chemischen Modifikation von Efsevin zur optimierten mitochondrialen Kalziumaufnahme geschlossen werden kann. Basierend auf dem Befund, dass in zwei der drei Untersuchungsmethoden messbare Unterschiede in der Wirksamkeit der Derivate beobachtet wurden, repräsentiert dieser Ansatz jedoch eine Optimierungsmöglichkeit der mitochondrialen Kalziumaufnahme. Aus diesem Grund stellen chemisch modifizierte mitochondriale Kalziumaufnahmeverstärker, ein wertvolles Forschungsziel für zukünftige Untersuchungen dar.

2 Introduction

2.1 Cardiovascular diseases

As of today, cardiovascular diseases (CVDs) represent a highly relevant health issue across the world. In the period from 2016 to 2017, CVDs accounted for 13% of the total US health expenditures³. Data from Europe recorded CVDs to be responsible for more than 126 million inpatient days and an overall cost of 169 billion euros in 2003⁴.

World Health Organization WHO states this group of disorders as leading cause of death worldwide for the previous 20 years⁵. Within nine years the number of deaths related to heart disease increased from 2 million to nearly 9 million in 2019⁶. Approximately 18 million people die from CVDs accounting for around one third of all global deaths every year⁷. Also, unlike almost all other causes of deaths, CVDs present a leading cause of death throughout high-, middle- and low-income populations⁸.

CVD cover a wide spectrum of etiologies. Alongside ischemic heart diseases and strokes, sudden cardiac death (SCD) is estimated to account for about 40-50% of overall cardiovascular deaths⁹. Cardiac arrhythmias, are predominantly observed as an underlying factor of SCD¹⁰. The most common cardiac rhythm disorder is atrial fibrillation (AF). Europe-wide AF presented in around 8.8 million adults above the age of 55 years in 2010. An estimate for its progression to 2060 is a rise to around 18 million

people affected. Estimations state a lifetime risk of atrial fibrillation in individuals of European descent to be around 1 in 3³.

In conclusion, cardiac arrhythmia are not only posing a financial issue to the health care system, but also adequate medical care and treatment of cardiac arrhythmia represent major challenges¹¹.

2.2 Electrophysiological principles of the heart and the origin of cardiac arrhythmia

2.2.1 Functional organization of the heart muscle

Our heart is a hollow muscle functioning like a pump. Its contractions maintain the blood circulation, supplying all tissues with oxygen and required nutrition. In order to pump blood through the body, a regular heart beat consisting of diastole and systole must be generated by heart muscle cells that have to be precisely coordinated in place and time¹². This process is based on electrical signals known as action potentials originating from the natural pacemaker center of the heart, the sinus node¹³. From there the electrical impulses travel via an excitation conduction systems along the myocardium to the ventricles until the entire ventricular myocardium is fully excited resulting in a contraction of the entire heart muscle¹⁴. The smallest subunit of the heart muscle are cardiomyocytes with a length of 0.1mm and a diameter of 20 μ m¹². They function as a network connected by gap junctions to optimize the propagation of cardiac excitation¹⁵.

2.2.2 Cardiac excitation-contraction coupling and intracellular calcium (Ca²⁺) signaling

The process of electrical activation via membrane depolarization in the heart resulting in a triggered contraction of cardiomyocytes is termed excitation-contraction coupling (ECC)¹⁶. As mentioned previously, the origin of each contraction initiating the systole is an electrical impulse, which propagates over the surface membrane of cardiomyocytes and reaches into cell invaginations called transverse-tubules, activating voltage-controlled L-type Ca²⁺ channels (LTCC) leading to an influx of Ca²⁺ (*Figure 1*). The entering Ca²⁺ induces a large Ca²⁺ induced Ca²⁺ release (CIRC) from the sarcoplasmic reticulum (SR) by activation of ryanodine receptors (RyR)^{17,18}. RyR2 is the cardiomyocyte-specific isoform of the ryanodine-receptor-family through which the SR releases Ca²⁺ into the intracellular space. The rise of intracellular free Ca²⁺ ([Ca²⁺]_i) allows Ca²⁺ to bind to troponin C leading to a myofilament contraction by enabling the connection between myosine heads and actine filaments forming a cross bridge formation^{16,19}. For relaxation during diastole, ([Ca²⁺]_i) levels need to return to resting conditions to allow Ca²⁺ to dissociate from troponin. Subsequent relaxation by removal of Ca²⁺ is performed via four main pathways²⁰. While the major fraction is actively pumped back into the SR under the consumption of ATP via the sarco/endoplasmic reticulum Ca²⁺-ATPase (SERCA), a small fraction of Ca²⁺ is extruded from the cell via

the sarcolemmal $\text{Na}^+/\text{Ca}^{2+}$ exchanger (NCX). NCX as cell membrane protein acts as antiporter importing three sodium ions in exchange of one exported Ca^{2+} ion to the extracellular space as the cardiomyocyte relaxes. Furthermore, also sarcolemmal Ca^{2+} ATPase and mitochondria are actively involved in the removal of cytosolic Ca^{2+} (Figure 2).

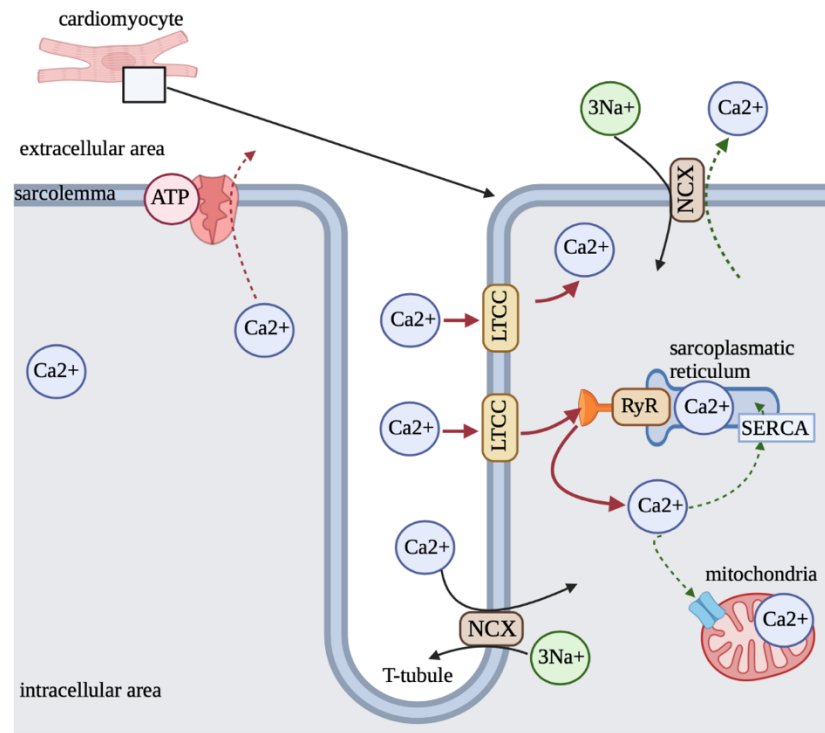


Figure 1: Schematic of Ca^{2+} signaling proteins and excitation-contraction coupling (ECC)

Ca^{2+} enters through the L-type Ca^{2+} channel (LTCC) and activates the ryanodine receptor (RyR) leading to a Ca^{2+} -induced Ca^{2+} release (CICR) out of the SR (red arrows). Ca^{2+} released from the internal store together with Ca^{2+} entering through the LTCC causes a rise in intracellular free Ca^{2+} . Ca^{2+} is then extruded from the cell via the $\text{Na}^+/\text{Ca}^{2+}$ exchanger (NCX), shuffled back into the SR via Ca^{2+} -ATPase (SERCA) or into mitochondria via the mitochondrial Ca^{2+} uniporter to return to basal Ca^{2+} levels (green arrows). [created with BioRender²¹]

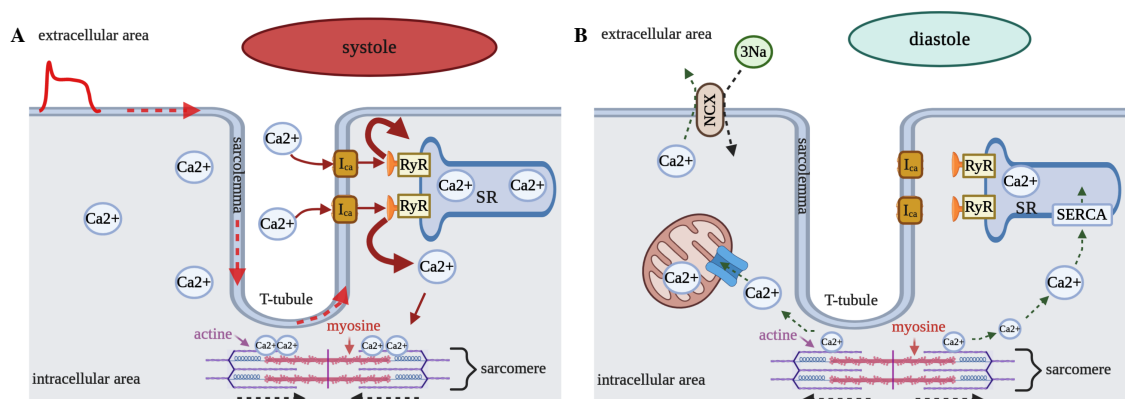


Figure 2: Schematic of Ca^{2+} signaling during systole and diastole

A) During systole, cell membrane is depolarized by electrical potential change (light-red arrows), Ca^{2+} enters through the L-type Ca^{2+} channel (LTCC), and activates the ryanodine receptor (RyR) to release the contents of the SR (dark-red arrows). Ca^{2+} released from the internal store together with Ca^{2+} entering from I_{Ca} causes a rise in intracellular free Ca^{2+} that can bind to troponin C (myofilaments) to cause contraction (black arrows).

B) For relaxation of the cardiac muscle cell during diastole, Ca^{2+} is then extruded from the cell via the $\text{Na}^+/\text{Ca}^{2+}$ exchanger (NCX), shuffled back into the SR via Ca^{2+} -ATPase (SERCA), or into mitochondria via the mitochondrial Ca^{2+} uniporter to return to basal Ca^{2+} levels (green arrows). [created with BioRender²¹]

2.2.3 Pathophysiology of arrhythmia and its pharmacological therapy

The pathogenesis of cardiac arrhythmias is highly variable and complex, and in many cases multiple arrhythmic mechanisms are intertwined. As complex as arrhythmic mechanism seem, in many cases the causality of arrhythmia is related to an imbalance of ion currents²². For example, a common mechanism is an increase in diastolic Ca^{2+} release, induced by pathologies such as heart failure, pathologies based on mutations of the ryanodine receptor (*Figure 3*), or SR Ca^{2+} overload. These erratic Ca^{2+} signals are the cellular trigger for arrhythmia mechanisms such as an accelerated automatism due to increased diastolic depolarization, the re-entry circuits or triggered activity by afterdepolarizations during or after cellular repolarization²³. A Ca^{2+} efflux through leaky RyRs triggers late after-potentials which favors reentry circuits establishing Ca^{2+} as a significant trigger of cardiac arrhythmias and a potential target of drug therapy.

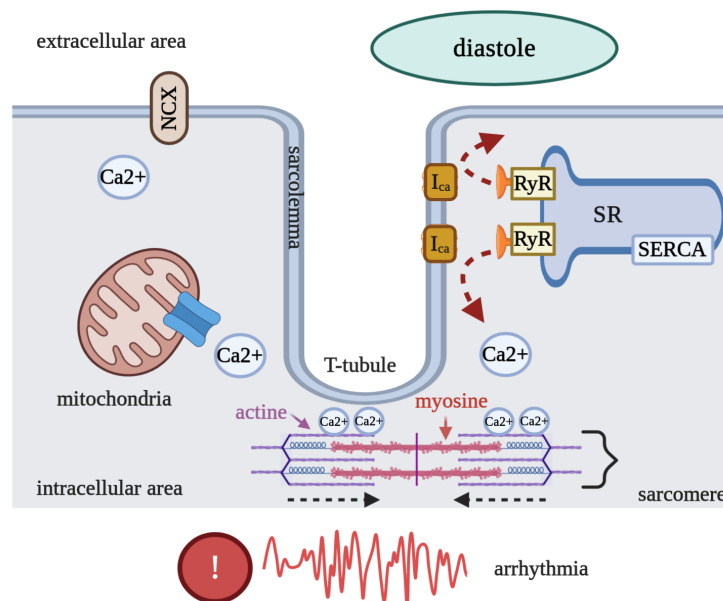


Figure 3: Schematic of intracellular Ca^{2+} release by leaky RyR resulting in cardiac arrhythmia

Leaky RyR can lead to Ca^{2+} release during diastole (dark-red arrows) and therefore spontaneous contractions (black arrows) occur during the relaxation phase leading to additional contractions causing arrhythmic events. [created with BioRender²¹]

Therapeutic approaches for the treatment of cardiac arrhythmia are limited and risky. In 1970 Vaughan Williams categorized antiarrhythmic drugs into four classes of medications according to their main mechanism of action²⁴: sodium-channel-blockers,

beta receptor-blockers, potassium-channel-blockers and Ca^{2+} channel antagonists. All of them are based on the ability to affect the electrical excitation of cardiomyocytes. This established classification was later modified by Donald C. Harrison²⁵ focusing on greater regard to clinical benefits. Despite a continuous growth of knowledge about their cellular electrophysiological effects these classifications are still commonly applied to currently used pharmaceuticals. However, as the majority of antiarrhythmic drugs cause an interruption of various cellular pathways, a clear assignment to one of these categories is often impossible. Additionally, other antiarrhythmic drugs, including adenosine or cardiac glycosides, cannot be classified into one of these initial groups, they can be found in more recent classifications²⁶.

Since most cardiac arrhythmias present permanent conditions, lifelong treatment is mostly necessary. However, in the majority of cases currently used antiarrhythmic drug therapy leads to proarrhythmic side effects in the long term²⁷ due to the effects on the action potential generation. This observation was already proven by several studies investigating certain drug groups resulting in insufficient long-term therapy²⁸. The Cardiac Arrhythmia Suppression Trial (CAST) performed in 1986 investigated the efficacy of class I antiarrhythmics on preventing sudden cardiac death after a heart attack, and revealed increased mortality from arrhythmias after treatment with certain drugs of this pharmacological group²⁹. Amiodarone, a versatile class III antiarrhythmic drug, which is widely used and considered to be highly effective for treatment of supraventricular and ventricular tachyarrhythmia, has a number of serious side effects affecting multiple organs³⁰. Thus, with the exception of β -blockers, none of the commonly used antiarrhythmics can be deployed for long-term treatment³¹. Therefore, surgical interventions such as ablation or the use of implantation of implantable cardioverter-defibrillators (ICDs) have become first-line therapy³², but long-term success rates are still insufficient.

Due to the potential of current drug therapy to induce proarrhythmic and adverse side effects, the demand for alternative pharmacological therapies is still present and urgent. Even though Ca^{2+} -dependent arrhythmia mechanism represent a promising target for antiarrhythmic drugs,, until now there is no therapeutic approach intervening in the intracellular Ca^{2+} balance. All of the previously mentioned drugs target plasmalemmal channels for restoration of the heart rhythm without directly modifying the intracellular Ca^{2+} -load. However, various experimental studies demonstrate intracellular Ca^{2+} increase as leading trigger of (ectopic) excitations³³. As there would be no impact on the cardiac conduction system but possible intracellular triggers of arrhythmia could be directly targeted within the cell, the intracellular Ca^{2+} system therefore appears to be a promising target in the search for antiarrhythmic drugs³⁴.

The intracellular concentration of free Ca^{2+} in a resting cardiomyocyte is approximately 10^{-7} M which is multiplied by a factor of 100 during excitation to approximately 10^{-5} M, whereby the level of extracellular Ca^{2+} is around 10^{-3} M³⁵. The SR is an intracellular organelle specialized in Ca^{2+} storing and cycling and therefore represents the main intracellular Ca^{2+} storage of cardiac myocytes located in close proximity to LTCCs. The extent to which the contractile apparatus is activated depends on the intracellular Ca^{2+}

concentration¹². An increased Ca^{2+} influx leads to a higher Ca^{2+} load of the SR resulting in increased cardiac strength. The Ca^{2+} metabolism of the heart and its correct balance correlates directly with cardiac performance, and defects in the Ca^{2+} homeostasis are consequently associated with potential heart pathologies/CVDs such as heart failure, cardiac dysrhythmia or hypertrophy^{36,37}.

2.3 Ca^{2+} signaling in cardiovascular diseases

As outlined above, Ca^{2+} is one of the major determinants of CVDs. Within the last decades Ca^{2+} and its role on heart function has been a focus of extensive research. An increased incidence of myocardial infarction³⁸, as well as irregular heart rhythms leading to cardiomyopathies and heart failure³⁹ showed a close association to abnormalities in Ca^{2+} regulation. Already in the late 90's alterations in Ca^{2+} proteins were described in the failing human heart, showing an involvement of SERCA and NCX⁴⁰. Shortly after, more evidence accumulated for a downregulation of SERCA levels in failing hearts partially compensated by an upregulation of NCX in dogs⁴¹. These findings provided potential novel therapeutic approaches in heart failure⁴². In around 80% of patients with congestive heart failure ventricular arrhythmia was recorded as a major underlying cause in subsequent sudden death⁴³. Sudden cardiac death in young patients with condition of catecholaminergic polymorphic ventricular tachycardia (CPVT) are also tightly linked to an imbalance of Ca^{2+} homeostasis. In CPVT, patients show *RYR2* mutations leading to diastolic Ca^{2+} leakage from the SR and therefore delayed afterpolarizations resulting in triggered arrhythmia⁴⁴. Mechanisms such as late and early afterdepolarizations demonstrate common causes for arrhythmic events^{45,46}, which again put Ca^{2+} proteins in a significant spotlight. Ca^{2+} handling therefore provides an important field in the prevention and therapy of various cardiovascular diseases.

Tightly linked with intracellular Ca^{2+} are mitochondria. Observations showed a small fraction of systolic Ca^{2+} is taken up by mitochondria during relaxation, on the one hand for the regulation of cellular metabolism and supply with energy and on the other for shaping the kinetics of the Ca^{2+} transients contributing to the regulation of contractile activity¹². This mechanism, however, has not yet been intensely investigated although recent studies have indicated that it has greater modulatory capabilities than initially expected⁴⁷.

2.4 Mitochondrial Ca^{2+} uptake as therapeutic approach in arrhythmia

Above all, mitochondria are known as “powerhouses of the cell” producing ATP through oxidative phosphorylation. Nevertheless, some earlier studies also demonstrated their ability to take up Ca^{2+} ⁴⁸. In recent years, two main subpopulations of mitochondria were described in cardiac tissue: Subsarcolemmal mitochondria (SSM) are located beneath the cell membrane and exhibit a limited degree of organization varying in size and shape, whereas interfibrillar mitochondria (IFM) are positioned in a strict arrangement between myofibrils. Presumably, SSM primarily provide ATP through the sarcolemma for the

transport of electrolytes and metabolites⁴⁹. On the other hand, IFM show close proximity to known Ca^{2+} release sites of the SR. IFM's tight bonding to the SR membrane demonstrates an increased Ca^{2+} uptake capability, indicating a fundamental role in Ca^{2+} cycling⁵⁰. Electron microscopic observation of rat ventricular myocytes demonstrate that the majority (90%) of Ca^{2+} release units (CRUs) of the junctional SR are located at a close distance of only about 37 nm from the mitochondria^{51,52}. In addition, transmission electronic microscope (TEM) reveal thin strands (tethers) connecting adjacent SR and outer mitochondrial membrane⁵³.

The physiological mitochondrial barrier supporting ion uptake and release consists of inner (IMM) and outer mitochondrial membrane (OMM). The OMM contains a high density of large mitochondrial porins called voltage dependent anion channels (VDACs)⁵⁴ and thus the common perception was for a long time that it is freely permeable for Ca^{2+} . In 2001 Shoshan-Barmatz et al. however provided evidence that the permeability of VDAC for Ca^{2+} is variable and regulated. They described Ca^{2+} binding sites on VDAC placing it in the primary focus of Ca^{2+} transport through the OMM (*Figure 4*)⁵⁵. Within the IMM, a Ca^{2+} -selective ion channel, the mitochondrial Ca^{2+} uptake complex (MCUC)⁵⁶ further transports Ca^{2+} in the matrix. The MCUC consists of several subunits such as MCU, EMRE, MICU1 and MICU2, which in precise coordination form a refined Ca^{2+} transfer mechanism^{57,58}.

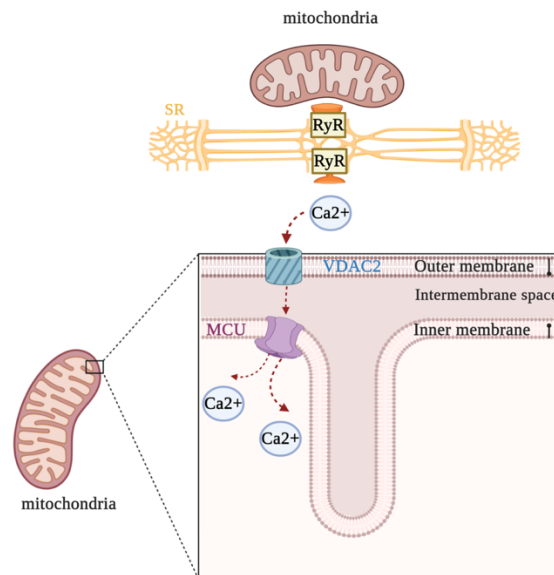


Figure 4: Schematic of cardiac mitochondrial Ca^{2+} transport represented by VDAC2 and MCU

Ca^{2+} extruded from the SR mediated by RyR enters mitochondria by first passing the OMM through VDAC crossing the intermembrane space and entering the inside of mitochondria by passing the IMM through MCU. [created with BioRender²¹]

As VDAC constitute the primary barrier of mitochondrial Ca^{2+} -uptake, this pore also displays great potential as a drug target.

2.4.1 Voltage dependent anion channel (VDAC) in mitochondrial Ca²⁺ transfer and antiarrhythmic treatment

In 1976 the first activity of voltage-dependent anion channels (VDACs) was discovered by Schein et al. in a planar lipid bilayers⁵⁹ focusing on its conductance and gating function. When the transmembrane potential is neutral VDAC is in a so-called “open”, high-conductance state. Conversely, at potentials around 20-30mV gating of the channel into various gating states can be observed⁶⁰. Today, it is known that VDACs represent a family of mitochondrial diffusion pores that are barrel shaped, have an internal diameter of approximately 2.5-3 nm and display a molecular weight of about 32-34kDa⁶¹⁻⁶⁵. VDAC consists of 19 β -sheets aligned in antiparallel formation with an α -helix at the N-terminus on the inside of the barrel (*Figure 5*). Animals and plants express three isoforms of VDAC. Purified VDAC reconstituted into liposomes or lipid bilayer showed high permeability to Ca²⁺. Channel binding sites as well as inhibition of Ca²⁺ transfer induced by lanthanides and RutheniumRed decreased channel conductance and inhibited Ca²⁺ accumulation in mitochondria⁵⁵. Moreover, VDAC2 was found to modulate diastolic Ca²⁺ sparks in HL-1 cardiomyocytes. In particular, knock-down of VDAC2 increased sparks duration, width and intensity. A significantly delayed mitochondrial Ca²⁺ uptake in these cells during artificial Ca²⁺ pulses indicated modulatory role of VDAC2 for cardiac local Ca²⁺ signaling⁶⁶.

2.4.2 Efsevin as promising mitochondrial Ca²⁺ uptake enhancer (MiCUp) in the treatment of cardiac arrhythmia

Targeting improved mitochondrial Ca²⁺ uptake, our lab recently identified a potent modulator of VDAC2 in cardiomyocytes. The synthetic compound efsevin, a dihydropyrrole carboxylic ester, was identified in a chemical screen on zebrafish embryos. Zebrafish embryos of the mutant line *tremblor*, which manifest uncoordinated irregular cardiac contractions due to a null-mutation in NCX⁶⁷, showed restored rhythmic cardiac contractions after treatment with efsevin¹. In translational models for catecholaminergic polymorphic ventricular tachycardia (CPVT) efficacy of efsevin was also proven⁶⁸. Efsevin suppressed arrhythmogenic events *in vivo* in CPVT mice as well as *in vitro* in induced pluripotent stem cell (iPSC)-derived cardiomyocytes from a CPVT patient using a planar lipid bilayer system containing *zVDAC2*⁶³, efsevin induced a shift towards the closed state of *zVDAC2*, which results in a transition to a lower anion-selectivity². Protein ligand docking in AutoDock Vina⁶⁹ was performed to further investigate the interaction between efsevin and *zVDAC2* on a molecular level. This approach revealed a binding pocket between the inner channel wall and the N terminal helix² (*Figure 5*).

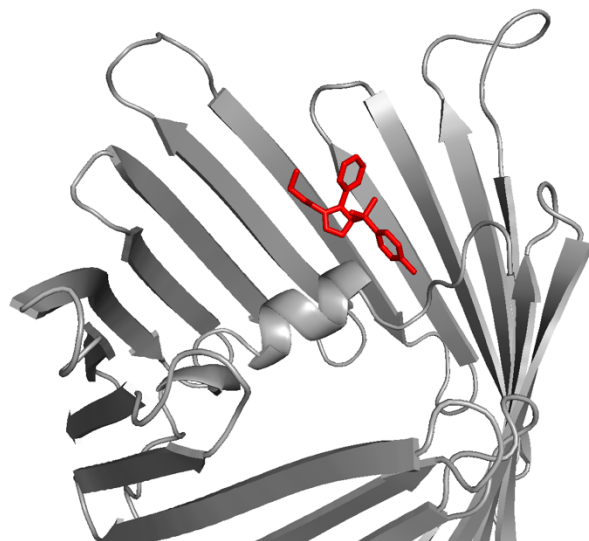


Figure 5: Predicted binding site of efsevin on zVDAC2 obtained in molecular docking²

Frontal view of efsevin (red) located in predicted binding site within the VDAC2 channel (grey, pdb:4bum) between N-terminal alpha-helix and inner channel wall.

In order to identify the most likely spatial position of the two molecular interactors, differing docking simulations were performed and revealed three prominent residues involved in drug binding interaction partners. Using a *zVDAC2* mutant in which these three partners were mutated to alanines, the binding pocket identified in molecular docking was experimentally confirmed. Furthermore, confirmatory results were obtained in HL-1 cardiomyocytes⁷⁰ depleted of the endogenous *VDAC2*, where overexpression of wild-type but not of the three alanine mutant of *zVDAC2* rescued SR-mitochondrial Ca^{2+} transfer².

This work clearly indicates that VDAC2 is an essential regulator of mitochondrial Ca^{2+} uptake in cardiomyocytes, which can be modulated by the substance efsevin, making it a promising drug target for cardiac arrhythmias.

However, the aforementioned HL-1 assay revealed a relatively high half-maximal activity of efsevin. Combined with a rapid hydrolyzation of efsevin in liver microsomes² these results suggest a very limited druggability of efsevin. Thus, though efsevin represents a leading candidate for the development of novel antiarrhythmics it requires prior optimization in order to become operational in clinical settings.

Therefore, my work addresses the question how chemical modification of efsevin could increase its efficacy, with the ultimate goal to create a potent drug against cardiac arrhythmias.

2.5 Aim and objectives

The aim of my work is the optimization of efsevin as a mitochondrial Ca^{2+} uptake enhancer (MiCU_p) for the treatment of cardiac arrhythmia.

Our collaboration partner created 40 chemically derivatives of efsevin. In a first step, the binding conformations and energies of these derivatives to VDAC2 were tested in an *in silico* approach using computational docking approach. In a second step, potency of these derivatives was investigated in an *in vivo* model: To this aim, the derivatives were ranked based on restoration of embryonic heartbeat using an arrhythmic zebrafish model. Lastly, I tested these derivatives in an *in vitro* model using HL-1 isolated cardiomyocytes to evaluate kinetics of SR-mitochondria Ca^{2+} transport of the most potent derivatives.

3 Material and Methods

3.1 Efsevin and its analogs

Efsevin and its analogs were designed and synthesized by Professor Ohyun Kwon at University of California, Los Angeles. The basic chemical structure of efsevin (*Figure 6*), a dihydropyrrole carboxylic ester compound, was modified into forty different derivatives (*Figure 7*) by mainly using the halogens chlorine, bromine and fluorine, as well as hydrogen. Chemical groups were attached, removed or shifted either at position C4', C5' or C6' of the first pyrrole or position C3'' and/or C4'' of the second pyrrole.

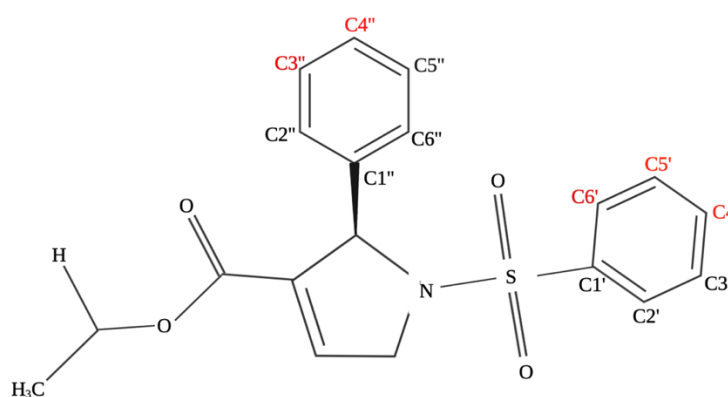


Figure 6: 2D-schematic of efsevin structure

Positions for variation of chemical groups: C4', C5' and C6' (of the first pyrrole) or C3'' and C4''. [created with BioRender²¹]

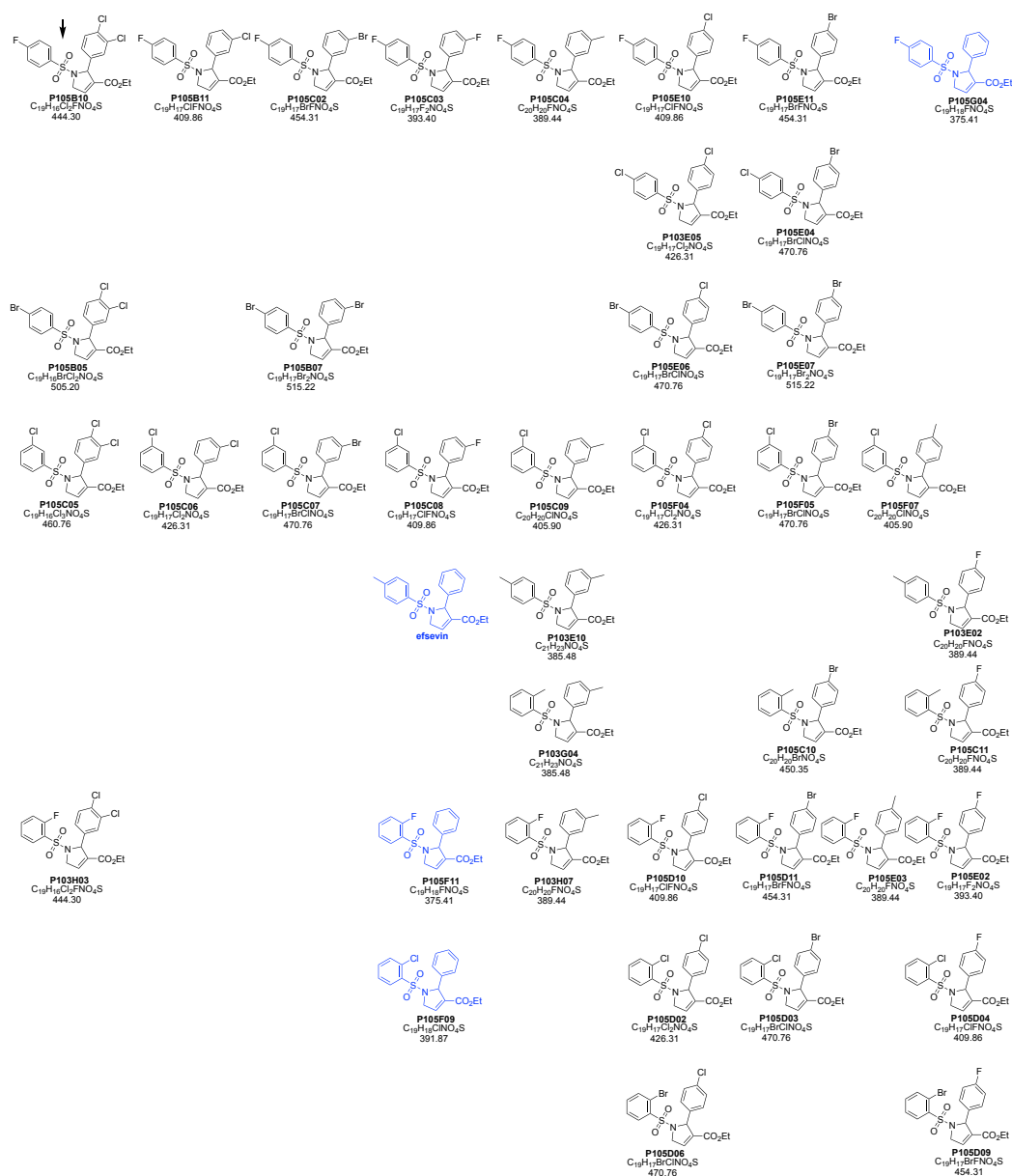


Figure 7: 2D-schematic of efsevin derivatives

Forty different compounds were generated by Professor Ohyun Kwon built on efsevin as the basic framework (designed by Professor Ohyun Kwon at University of California, Los Angeles).

3.2 Molecular docking

3.2.1 Docking process

To perform molecular docking, three-dimensional structures of all efsevin analogs were generated using MarvinSketch⁷¹ and saved in protein data bank (.pdb) format. Via the Research Collaboratory for Structural Bioinformatics protein data bank (PDB) the crystal structure of *zVDAC2* (PDB ID: 4BUM) as molecular interaction partner for the compounds was obtained. After generation of protein and ligand, AutoDockTools (v1.5.6)⁷² was used to add Gasteiger charges and hydrogens for molecular docking. Dockings were subsequently performed using AutoDockVina⁶⁹. Side chains of the interaction site (N19, Y22, F24, N207, R218, K236, N238, L242, L262) were maintained flexible for the entire docking process, the grid box was narrowed down to 24 Å x 20 Å x 20 Å² around the binding site and each docking was performed with an exhaustiveness level of 8. Each substance was tested in five consecutive dockings and the respective predicted affinities (kcal/mol) were documented (*Figure 8*). Each run generated nine distinct and probable dockings independent from the previous one.

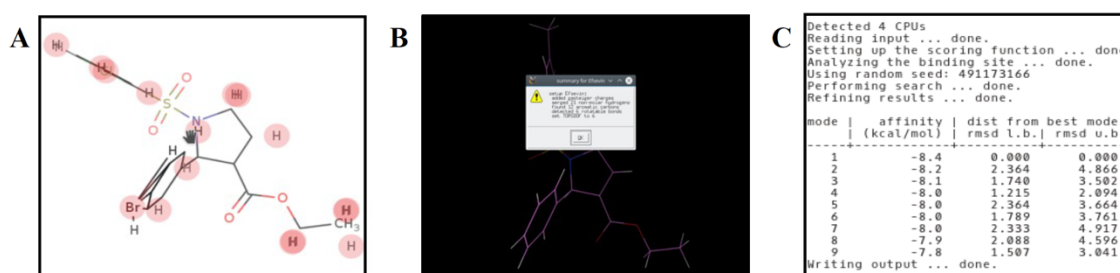


Figure 8: Docking process: efsevin and VDAC2 as ligands

(A) Three-dimensional structure of efsevin generated in MarvinSketch, (B) Gasteiger charges and hydrogens added by AutoDockTools for docking process, (C) results of performed docking using efsevin and VDAC2 as ligands in AutoDock Vina.

3.2.2 Docking analysis/evaluation/ranking

For the screening of efsevin analogs and their binding affinities towards VDAC2, a scoring system was developed. For the analysis of the interactions only affinities (kcal/mol) of values higher than 7 were considered. Affinities of ≥ 8 scored ten points, affinities of 7.5 to 7.9 scored four points, and affinities of 7.0-7.4 scored one point. Thereafter, points from a total of 45 dockings for each derivative were summed up and the results were ranked. As negative control, four dockings with the inactive efsevin analogon OK-C19^{LB1} were performed.

3.3 Zebrafish experiments

Zebrafish (*Danio rerio*) of the line *tremblor* (*tre^{tc318}*); TG(*cmlc2*:GFP) were received from Jau Nian Chen, PhD, Department of Molecular, Cell and Developmental Biology at UCLA. Heterozygous zebrafish were maintained and raised as described by Westerfield⁷³. Homozygous *tre^{tc318}* mutant embryos are characterized by a loss of function in the cardiac specific Na⁺/Ca²⁺ exchanger 1 (NCX1h), causing a Ca²⁺ extrusion defect in cardiomyocytes⁶⁷. As a result, embryonic hearts contract uncoordinatedly, phenotypically resembling fibrillation in human hearts. To enable a more detailed investigation of heart function such as cardiac contractility and rhythmicity, the *cmlc2*:GFP transgene drives the expression of green fluorescent protein (GFP) in cardiomyocytes⁷⁴.

3.3.1 Zebrafish phenotype rescue experiment

To test the effects of efsevin derivatives on restoration of rhythmic heart beats we first obtained homozygous *tremblor* zebrafish embryos by crossing heterozygous *tremblor* adult zebrafish⁶⁷. Therefore, zebrafish were divided around 7 days prior to the crossing into males and females to increase the spawning readiness. In the evening, one male and one female fish were transferred into a crossing cage and separated by a transparent disk. In the following morning, disks were removed for a spawning period of approximately 30 minutes to ensure a synchronized development of the embryos. Afterwards approximately 8 hours post fertilization (hpf), eggs were collected and stored in E3 buffer containing NaCl (5mM), MgSO₄ x 7H₂O (0.33mM), KCl (0.17mM) and CaCl₂ x 2H₂O (0.33mM) at 28°C. Around 100-150 embryos for each condition were transferred to a 6-well-plate in 2000µl E3 buffer. To examine the impact of the different efsevin derivatives on the rhythmicity of the *tremblor* heartbeat phenotype, 20µM of either the tested derivative, efsevin (as positive control) or dimethyl sulfoxide (DMSO, as a vehicle control) were added. The eggs were incubated at 28°C overnight. To enable an unobstructed uptake of the substances and an easier microscopic screening, embryos were dechorionated approximately 25 hpf by adding 30 µg/ml protease (derived from *Streptomyces griseus*) to the respective buffer mixture. After approximately 10 minutes chorions were digested and hatched embryos were transferred to a new 6-well-plate containing E3 buffer supplemented with test substances. Embryos were exposed to the test substances for an additional time of 6 hours at 28°C to ensure optimal absorption by the organism. At 30-32 hours post fertilization the function and rhythmicity of the embryonic *tremblor* heart was analyzed using a fluorescence binocular light microscope. During the first scoring, embryos were differentiated into two groups, depending on their rhythmic and non-rhythmic cardiac contractions (regardless of heartrate). Both groups were again incubated at 28°C in renewed E3 buffer without the test substances overnight. On the next day, (48 hpf) the embryos' heartbeats were analyzed in a second scoring (*Figure 9*). Embryos which demonstrated synchronized contractions on the first scoring at 30hpf treated with substance but then displayed arrhythmic or no contraction after removal of the derivatives in the rescoring were considered rescued *tremblor*. The ratio

of rescued *tremblor* embryos over total *tremblor* embryos was calculated to have a measure for the anti-arrhythmic effect of the tested derivatives.

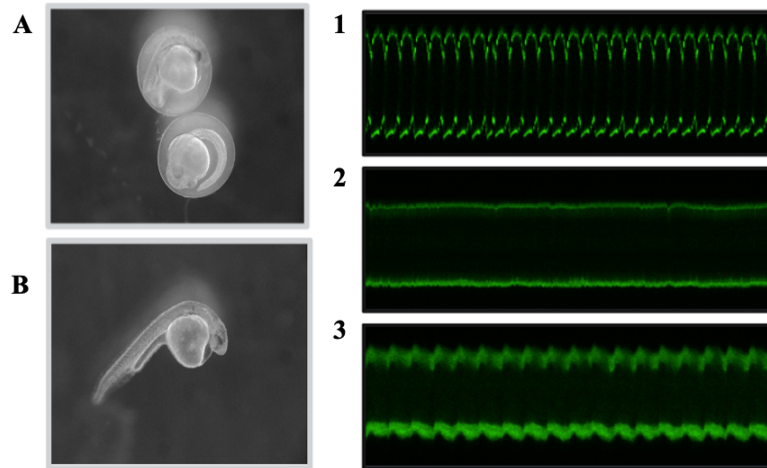


Figure 9: *In vivo* approach to measure efsevin's effect on heart arrhythmia

(A) and (B) Images of zebrafish embryos taken with a binocular light microscope (A) two zebrafish embryos 25 hpf prior to dechorionisation, (B) dechorionated zebrafish embryo 25 hpf.

(1) – (3) GFP- tagged zebrafish heart line scans at 48 hpf recorded with a confocal microscope (1) wild-type zebrafish embryo displaying frequent and synchronized systoles and diastoles, (2) vehicle *tremblor* embryonic heart displaying sporadic and unsynchronized systoles and diastoles, (3) efsevin-treated *tremblor* embryonic heart displaying frequent and regular contractions.

3.4 HL-1 cells

In order to provide a direct comparison of the effect of derivatives on mitochondrial Ca^{2+} uptake, I used a mitochondrial Ca^{2+} uptake assay in HL-1 cardiomyocytes, allowing quantification of direct Ca^{2+} transfer between SR and mitochondria.

The HL-1 cardiac cell line was first obtained from an AT-1 mouse atrial tumor in 1998 by Dr. William Claycomb (Louisiana State University)⁷⁰. The HL-1 cells used in these experiments were a donation by Dr. Claycomb.

3.4.1 HL-1 cardiomyocyte culture

The media listed below were used to culture HL-1 cells.

Supplemented Claycomb Medium

Reagent	Final concentration
Claycomb Medium (Sigma)	87%

Fetal bovine serum (batch tested and recommended by Sigma for HL-1 culture)	10%
Penicillin/Streptomycin	100U/ml; 100µg/ml
L-Glutamine	2 mM
Norepinephrine	0.1 mM

Claycomb Wash Medium

<u>Reagent</u>	<u>Final concentration</u>
Claycomb Medium	94%
Fetal bovine serum (HL-1 specific)	5%
Penicillin/Streptomycin	100U/ml; 100µg/ml

Freshly thawed cells were treated with 5µl plasmocin (25µg/ml) for 2 weeks to prevent mycoplasma contamination before experiments. HL-1 cells were fed with supplemented Claycomb Medium every weekday (5 ml / T-25 flask). Over the weekend HL-1 cells were supplied with double the amount of medium (10 ml / T-25 flask). Before passaging, T-25 flasks (1 ml) and 96-well plates (50 µl per well) were coated by adding sterile 0.02% gelatin and 0.1% fibronectin and incubated for at 37°C at least one hour prior to the split. The gelatin and fibronectin coating were removed by aspiration just before cells were added. Cells with 100% confluency were split 1:2 on Monday and Wednesday and 1:3 on Friday. All reagents used for the split were preheated to 37°C. To eliminate cell debris and dead cells, HL-1 cells were gently washed with 3 ml of phosphate buffered saline (PBS) before being treated with 1 ml of 0.05% trypsin/EDTA to detach the cells for 1 minute. To complete the detachment of the cells, 1 ml of trypsin/EDTA was renewed for an additional period of 2 minutes at 37°C. Afterwards, the reaction was inactivated by soybean trypsin inhibitor (0.05%). The total suspension of 2 ml was transferred to a 15 ml tube. The T-25 flask was washed with 5 ml Claycomb Wash Medium to remove remaining cells and added to the 15 ml tube, followed by 5 minutes centrifugation at 500 x g. The supernatant was removed by aspiration and the cell pellet was cautiously re-suspended in Full Claycomb Medium. Finally, in a 1:2 split, half of the suspension was transferred to a new T-25 flask containing supplemented Claycomb Medium, while the second half was used for experiments.

3.4.2 Mitochondrial Ca²⁺ uptake measurements

Fluorescence-based measurements of mitochondrial Ca²⁺ were performed on permeabilized HL-1 cells to quantify direct transfer of Ca²⁺ from the SR into mitochondria using the following solutions.

External solution (pH: 7.4 NaOH; 37°C)

Reagent	Final concentration (in mM)
NaCl	140
KCl	6
CaCl ₂	2
MgCl ₂	1
Glucose	10
HEPES	20

Ca²⁺ free external solution (pH: 7.4 NaOH; 37°C)

Reagent	Final concentration (in mM)
NaCl	140
KCl	6
MgCl ₂	1
Glucose	10
HEPES	20

Internal solution (pH: 7.2 Trizma base; 37°C)

Reagent	Final concentration (in mM)
BAPTA	1
HEPES	20
K-Asp	100
KCl	40
MgCl ₂	0.5

Malicacid	2
Glutamicacid	2
Pyruvatacid	5
Mg-ATP	5
CaCl ₂	0.47 [~ 100nM free Ca ²⁺] (*)
KH ₂ PO ₄	0.5

(*) based on calculation on „WEBMAXC STANDARD“⁷⁵

HL-1 cells were plated 26 hours prior to experiments on a 96-well plate at a density of 22.000-25.000 cells per well and incubated at 37°C and 5% CO₂. 4 µM Rhod-2, AM, a cell permeable, Ca²⁺ sensitive fluorescent dye, that preferentially accumulates in mitochondria due to its highly negative potential, was added at 37°C together with 0.08% of Pluronic F-127, a bio reagent that is non-ionic and assists the nonpolar acetoxymethyl (AM) ester Rhod-2 to pass the cell membrane. Afterwards, cells were incubated with external solution for 20 minutes at 37°C for de-esterification of the dye and an additional washing with Ca²⁺ free external solution was performed to eliminate remaining Ca²⁺ traces. Cells were permeabilized with 25 µM digitonin in internal solution for 3 minutes to remove cytosolic dye and ensure a specific mitochondrial fluorescent signal. Cells were washed three times in 1.5 minutes intervals with internal solution immediately after permeabilization. Then, the impact of efsevin derivatives on SR-mitochondrial Ca²⁺ transfer was examined by adding the compounds in various concentrations to the internal solution 4.5 minutes prior to the measurements. DMSO was used for vehicle control. Each analog was tested with efsevin as a positive control and a negative control with 10 µM of Ruthenium Red (RuR), an inhibitor of the mitochondrial Ca²⁺ uniporter (MCU) located in the inner mitochondrial membrane to ensure a specific mitochondrial signal. Ca²⁺ transfer measurements were performed with Infinite® 200 PRO multimode reader (Tecan, Maennedorf, Switzerland). For each experiment prior to the measurement, adjustment of the Z-position of the plate reader was performed to obtain the best possible signal. Rhod-2 fluorescence was continuously measured to monitor mitochondrial Ca²⁺ over 60 seconds at excitation wavelength of 540 (+/- 9) nm and emission wavelength of 580 (+/-20) nm. After 20 seconds, 10 mM caffeine were injected to induce ryanodine receptor mediated Ca²⁺ release from the SR, and to measure the resulting increase of mitochondrial Ca²⁺ uptake (*Figure 10*). Within each run 4 wells were treated and measured simultaneously.

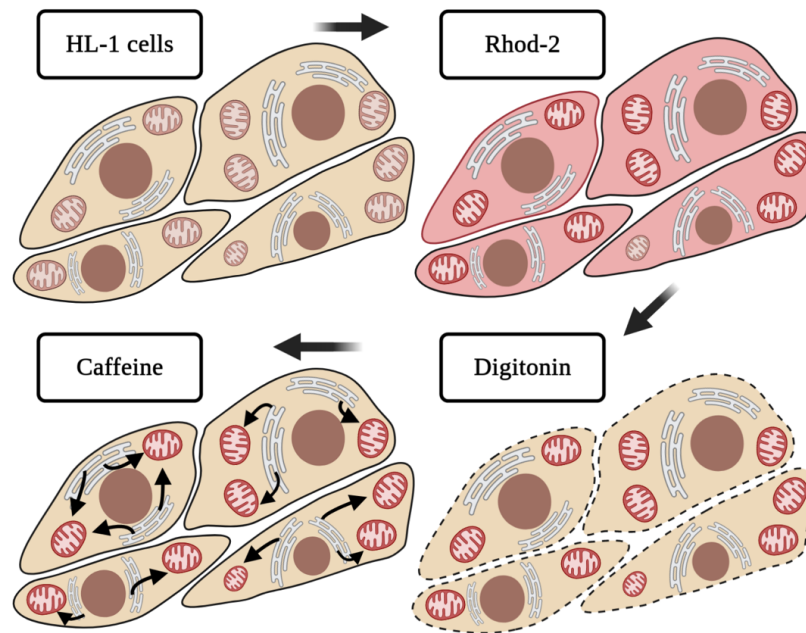


Figure 10: Schematic of HL-1 assay

HL-1 cells were stained with 4 μM of Rhod-2 (red coloring), afterwards permeabilized with 25 μM of digitonin (dashed line) to eliminate cytosolic dye. For RyR-initiated Ca^{2+} release out of the SR (black arrows) 10mM caffeine was injected. [created with BioRender²¹]

3.5 Evaluation methods

3.5.1 Statistical analysis

Data are expressed as mean \pm SEM. Statistical tests applied: unpaired T-test, oneway ANOVA-Test, 2way ANOVA test. Significance level was set at $*=p<0.05$; $**=p<0.01$; $***=p<0.001$, $****=p<0.0001$.

3.5.2 Graphical presentation

For presentation of graphs Libre Office Calc 4.3, Graphpad, Inkscape and Microsoft PowerPoint 12.3.6 were used.

4 Results

4.1 Screening of efsevin derivatives using computational docking

Using molecular docking, a binding pocket of VDAC2 was previously identified as binding site of efsevin². Here this method was adopted to perform a screening approach for new efsevin analogs in order to evaluate their efficiency. Each analog was docked into the VDAC2 binding pocket. The developed scoring system was used to evaluate binding affinities from 45 independent conformations from 5 docking runs for each substance. Surprisingly, efsevin still showed the highest binding affinity with a total score of 252 out of a possible score of 450. Derivatives P103E02 and P103E05 scored above 200 points, placing in the top performing derivatives in terms of affinity. 5 analogs scored within 150 and 200 points, three within 100-150 points and four derivatives scored between 75-100 points. 14 out of 40 derivatives scored lower than the negative control OK-C19¹ (*Figure 11*).

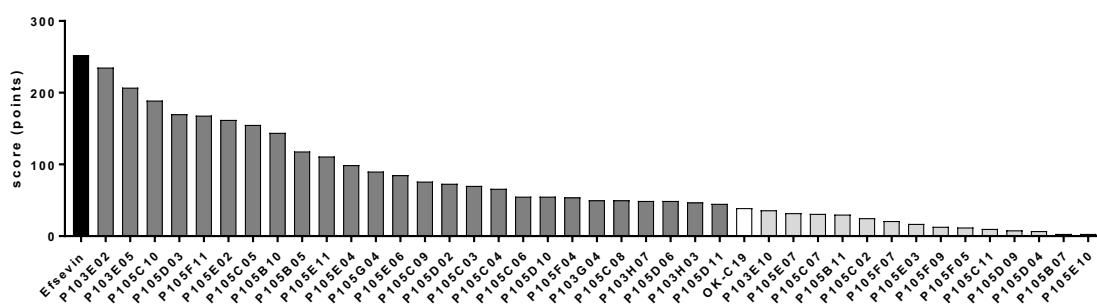


Figure 11: Efsevin showed highest binding affinity in computational docking screening

Efsevin and derivatives were scored based on their binding affinities (kcal/mol) in 45 independent conformations performed in 5 subsequent docking runs and set in relation. Four docking runs were performed with OK-C19.

For further analysis, derivatives with their various chemical groups were listed and sorted according to the affinity obtained in the docking simulations. By visually comparing visualized chemical modifications of the derivatives focusing on the two pyrroles no clear arrangements or chemical similarities between the derivatives according to their binding affinities could be determined (*Table 1*).

Rank	Compound	C2'	C3'	C4'	C5'	C6'		C2''	C3''	C4''	C5''	C6''
1	Efsevin			C								
2	P103E02			C						F		
3	P103E05			Cl						Cl		
4	P105C10					C				Br		
5	P105D03					Cl				Br		
6	P105F11					F						
7	P105E02					F				F		
8	P105C05				Cl				Cl	Cl		
9	P105B10			F					Cl	Cl		
10	P105B05			Br					Cl	Cl		
11	P105E11			F						Br		
12	P105E04			Cl						Br		
13	P105G04			F								
14	P105E06			Br						Cl		
15	P105C09				Cl				C			
16	P105D02					Cl				Cl		
17	P105C03			F					F			
18	P105C04			F					C			
19	P105C06				Cl				Cl			
20	P105D10					F				Cl		
21	P105F04				Cl					Cl		
22	P103G04					C			C			
23	P105C08				Cl				F			
24	P103H07					F			C			
25	P105D06					Br				Cl		
26	P103H03					F			Cl	Cl		
27	P105D11					F				Br		
28	P103E10			C					C			
29	P105E07			Br						Br		
30	P105C07				Cl				Br			
31	P105B11			F					Cl			
32	P105C02			F					Br			
33	P105F07				Cl							
34	P105E03					F				C		
35	P105F09					Cl				C		
36	P105F05				Cl					Br		
37	P105C11					C				F		
38	P105D09					Br				F		
39	P105D04					Cl				F		
40	P105B07			Br					Br			
41	P105E10			F						Cl		

Table 1: Derivatives display no clear correlations between the location and type of the chemical modifications and binding affinities obtained in computational screening

Efsevin and its derivatives were visualized focusing on their chemical structures and modifications [C(carbon), Cl(chloride), F(fluorine), Br(bromine)] within the two pyrrols (marked red). By using the scoring results of the computational docking screening derivatives were ranked by their affinities to binding pocket comparing chemical functional attachments showing no clear correlations.

Results revealed no superiority of any compound in comparison to efsevin in terms of obtained affinity to the binding pocket. Therefore, I performed a second screening approach using an *in vivo* method.

4.2 *In vivo* screening of derivatives performing phenotype rescue experiment in zebrafish embryos

As a second screening approach for efsevin analogs a zebrafish phenotype rescue assay was chosen. Efsevin was previously demonstrated to restore rhythmic cardiac contractions in embryos of the mutant line *tremblor*¹. To determine a standardized concentration for testing of derivatives against efsevin, rescuing effects of different concentrations of efsevin were determined using concentrations of 10 μ M, 20 μ M and 40 μ M (Figure 12). As control group, embryos treated with the vehicle DMSO showed a rescue ratio of 6.9% (\pm 2.0). Treatment with 20 μ M of efsevin showed the highest rescue ratio in embryos [61.4% (\pm 4.47), p <0.0001], compared to 10 μ M [28.0% (\pm 5.07), p <0.001]. Embryos treated with 40 μ M of efsevin displayed major phenotypic dysmorphologies and experiments were discontinued after the first experiment (27.3% rescue).

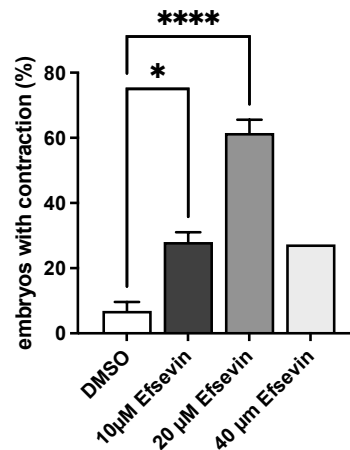


Figure 12: 20µM efsevin lead to highest rescue of rhythmic cardiac contractions in tremblor zebrafish embryos

Tremblor zebrafish embryos were treated with 10 µM (n=2), 20 µM (n=3) and 40 µM (n=1) of efsevin and DMSO (n=4) between 8hpf to 30 hpf and synchronized cardiac contractions were visually quantified. 10 µM ($p<0.001$) and 20 µM ($p<0.0001$) of efsevin displayed a significantly higher rescue rate than zebrafish embryos treated with DMSO. One batch of embryos treated with 40 µM displayed 27% higher rescue but this experiment was not repeated due to major dysmorphologies.

Next, the same experiment was performed with all forty derivatives at a concentration of 20 µM. Each condition was performed at least three times and each experimental run included efsevin and DMSO as a positive and negative control, respectively. Derivatives were ranked according to their quantitative rescue ability in percent (%) (*Figure 13*). Five substances that performed either superior or similar when compared to efsevin were identified including following derivatives: P105D03, P105E04, P105C10, P105B10 and P105F11. Whereas P105F11 [57.0% (± 6.17), n=5], P105B10 [57.4% (± 8.09), n=5], P105C10 [57.9% (± 5.34), n=5] and P105E04 [63.2% (± 6.45), n=6] marginally exceeded the rescue ratio of efsevin, the derivative P105D03 [76.3% (± 5.02), n=6, $p<0.01$] demonstrated a significant increase in the number of rescued embryos by 1.42-fold compared to efsevin. Further, none of the tested derivatives displayed any significant effects on growth and development of the embryos. Throughout the exposure to substances, all embryos were visually inspected regularly to detect indications of toxic or adverse effects.

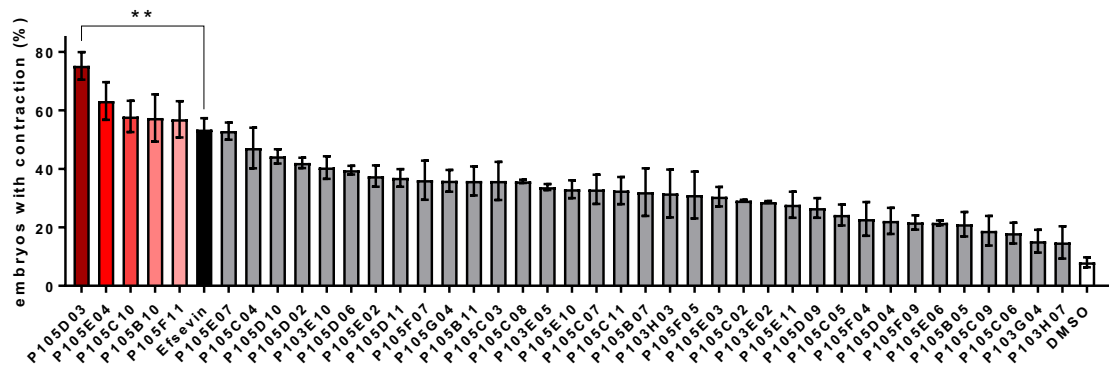


Figure 13: P105D03 significantly increases rescue of rhythmic cardiac contractions in *tremblor* zebrafish embryos

Tremblor zebrafish embryos were treated with DMSO (n=10), efsevin (n=16) and derivatives between 8hpf to 30 hpf, and synchronized cardiac contractions were quantified and ranked. Five substances scored higher than efsevin, with P105D03 (n=6) displaying statistical significance ($p < 0.01$).

Next, the functional groups of the derivatives based on the data obtained in the phenotype rescue screening in *tremblor* zebrafish embryos were again ranked and analyzed (Table 2). Also here, no affiliation or chemical similarity among any of the derivatives was evident.

Rank	Compound	C2'	C3'	C4'	C5'	C6'	C2''	C3''	C4''	C5''	C6''
1	P105D03					Cl			Br		
2	P105E04			Cl					Br		
3	P105C10					C			Br		
4	P105B10			F				Cl	Cl		
5	P105F11					F					
6	Efsevin			C							
7	P105E07			Br					Br		
8	P105C04			F				C			
9	P105D10					F			Cl		
10	P105D02					Cl			Cl		
11	P103E10			C				C			
12	P105D06					Br			Cl		
13	P105E02					F			F		
14	P105D11					F			Br		
15	P105F07				Cl				C		
16	P105G04			F							
17	P105B11			F				Cl			
18	P105C03			F				F			
19	P105C08				Cl						
20	P103E05			Cl					Cl		
21	P105E10			F					Cl		
22	P105C07				Cl						
23	P105C11					C			Br		
24	P105B07			Br					Br		
25	P103H03					F			Cl		
26	P105F05				Cl				Cl		
27	P105E03					F			Br		
28	P105C02			F					C		
29	P103E02			C					Br		
30	P105E11			F					F		
31	P105D09					Br			Br		
32	P105C05				Cl				Cl		
33	P105F04				Cl				Cl		
34	P105D04					Cl			Cl		
35	P105F09					Cl			F		
36	P105E06			Br					Cl		
37	P105B05			Br					Cl		
38	P105C09				Cl				C		
39	P105C06				Cl				Cl		
40	P103G04					C			C		
41	P103H07					F			C		

Table 2: Derivatives show no chemical similarity according to their potency of cardiac rhythmicity rescue in *tremblor* zebrafish

The functional groups of efsevin and the derivatives [C(carbon), Cl(chloride), F(fluorine), Br(bromine)] attached to the two pyrroles (marked red) were ranked according to their rescue ratio obtained from screening zebrafish *tremblor* embryos. The results revealed no correlation between their potency and chemical structure.

4.3 Quantification of SR-mitochondria Ca^{2+} transfer in HL-1 cardiomyocytes

After performing two different screening approaches, a third approach was used to explore the derivatives potency of the most active derivatives as mitochondrial Ca^{2+} uptake enhancer (MiCUp) in more detail. For measurement of direct Ca^{2+} transfer between SR and mitochondria, I used a mitochondrial Ca^{2+} uptake assay performed in HL-1 cardiomyocytes. Fluorescence-based measurement and quantification of mitochondrial Ca^{2+} following staining and permeabilization of HL-1 cardiomyocytes was performed after caffeine injection. To adapt this assay for the use with the identified derivatives, I first set out to reproduce previously obtained efsevin effects on mitochondrial Ca^{2+} uptake⁶⁸. Results successfully demonstrated an enhanced Ca^{2+} transfer by efsevin peaking at 10 μM (Figure 14). To examine the dose-dependent effects of efsevin in HL-1 cardiomyocytes and to optimize test concentrations, a dose-response curve of efsevin was generated demonstrating a B_{max} of 220% and EC_{50} of 4.4 μM . The highest efficacy was shown by efsevin at a dose of 10 μM . Importantly, Ca^{2+} uptake was suppressed by application of RuR indicating a specific mitochondrial Ca^{2+} uptake. (Figure 14 - 16)

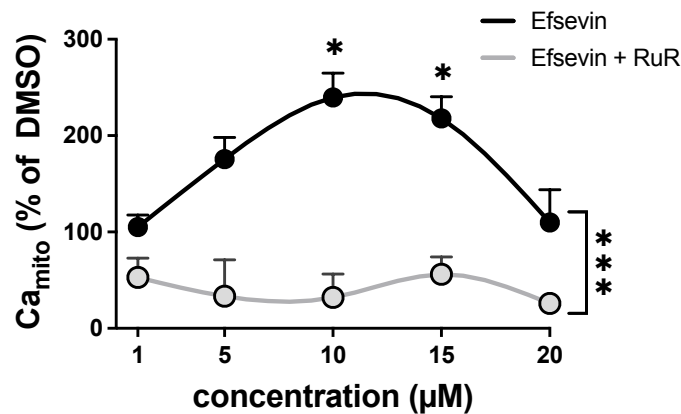


Figure 14: Dose-dependent mitochondrial Ca^{2+} uptake (in %) by efsevin in HL-1 cardiomyocytes

Mitochondrial Ca^{2+} uptake in the presence of efsevin was quantified in % in relation to the control group using DMSO (n=54). Efsevin (black values) showed dose-dependent enhancement of mitochondrial Ca^{2+} uptake measured at concentrations of 1 μM (n=9), 5 μM (n=9), 10 μM (n=29), 15 μM (n=27, $p=0.0016$) and 20 μM (n=3) reaching its peak at 10 μM ($p<0.0001$) and continuing in a plateau phase until 15 μM ($p=0.0016$). Mitochondrial Ca^{2+} uptake was sufficiently blocked by 10 μM RuR (grey values). (2way ANOVA; $F(1,96) = 14,92$, $p=0,0002$ Sidak's multiple comparisons test)

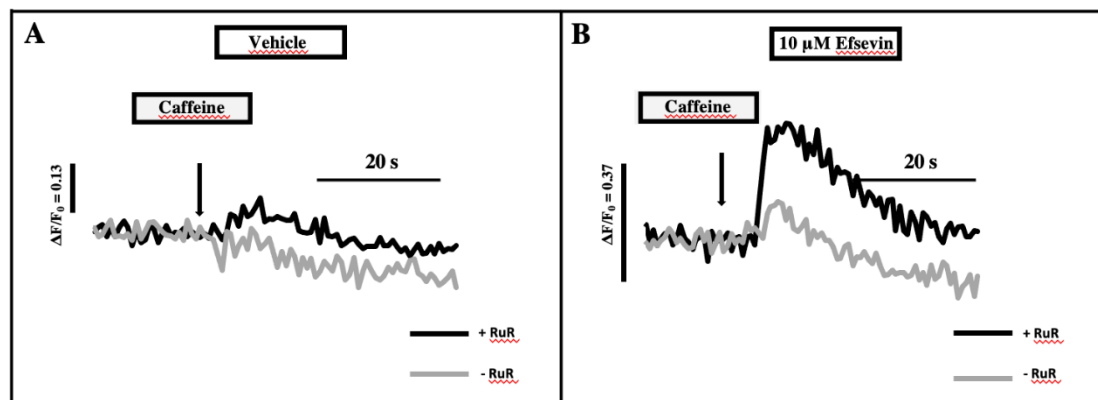


Figure 15: SR-mitochondria Ca^{2+} transfer in HL1-cardiomyocytes

Mitochondrial Ca^{2+} recordings from caffeine-induced SR Ca^{2+} release in permeabilized HL-1 cells. **(A)** Traces of vehicle application as control condition using DMSO (black) and in the presence of 10 μM RuR (grey) blocking mitochondrial Ca^{2+} uptake are shown. **(B)** Traces of 10 μM efsevin application (black) and in the presence of 10 μM RuR (grey) showing efsevin induced increase in mitochondrial Ca^{2+} uptake.

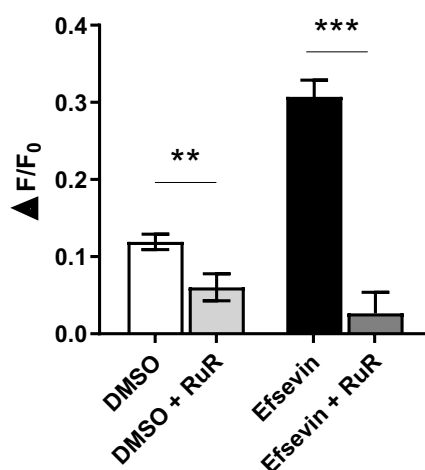


Figure 16: Statistical analysis of SR-mitochondria Ca^{2+} transfer in HL-1 cardiomyocytes

Permeabilized HL-1 cardiomyocytes showed a rise in Ca^{2+} -induced fluorescence change ($\Delta F/F_0$) after caffeine injection displaying an increase in mitochondrial Ca^{2+} uptake. Whereas control group (white) showed a rise of 0.12 ($\Delta F/F_0$) (n=54), that is suppressed to 0.06 ($\Delta F/F_0$) (n=18) by 10 μM RuR (grey) [$p < 0.01$], HL-1 cardiomyocytes displayed an efsevin-induced increase (black) in mitochondrial Ca^{2+} uptake of 0.30 ($\Delta F/F_0$) (n=29) [$p < 0.001$], that is suppressed to 0.03 ($\Delta F/F_0$) (n=10) by 10 μM RuR (grey).

Next, the effect of three selected derivatives (P105B10, P105D03 and P105E04) on SR-mitochondria Ca^{2+} transfer was evaluated. The selection of the derivatives was based on several aspects that were obtained in previous screenings: 1) a significant improvement of the rescue ratio in the *in vivo* trial, 2) a binding-affinity of more than 90 points referring to the scoring system in the computational screening, and 3) derivative composition of different chemical structures to ensure a heterogeneous selection. The highest scored

derivative in the zebrafish assay and rank 5 in the docking ranking with a score of 170 points was P105D03 containing a bromine atom at C4'' and a chloride atom at C6' molecule. P105E04 scored second best in the zebrafish ranking and rank 12 in the docking ranking with a score of 99 points was selected having a variant position of the chloride atom (C4') and a bromine atom (C4''). The final derivative selected was P105B10 which scored place 5 in zebrafish ranking and 9 in the chemical assay with a score of 144 presenting with three molecules, one fluorine (C4') and two chloride atoms (C3'' and C4''). For each derivative a dose-response curve was generated in order to provide a B_{max} and EC_{50} (Figure 17). Surprisingly, all three compounds resulted in improved EC_{50} values compared to efsevin. B105B10 ($0.27\mu\text{M}$), P105D03 ($0.61\mu\text{M}$) and P105E04 ($0.85\mu\text{M}$). Efsevin EC_{50} resulted in $4.4\mu\text{M}$.

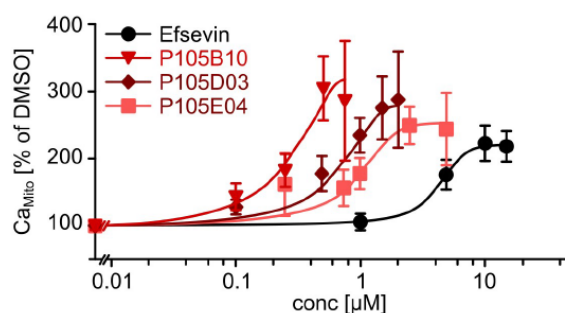


Figure 17: Derivative P105B10 displayed most efficient mitochondrial Ca^{2+} uptake in HL-1 cardiomyocytes

SR-mitochondria transfer was quantified by peak mitochondrial fluorescence in response to caffeine-induced SR Ca^{2+} release. P105D03, P105B10, P105E04 were dose-dependently analyzed in HL-1 cardiomyocytes. P105B10 showed highest pharmacological efficacy ($B_{max}=298\%$, $EC_{50}=0.27\mu\text{M}$) followed by P105D03 ($B_{max}=293\%$, $EC_{50}=0.61\mu\text{M}$), P105E04 ($B_{max}=247\%$, $EC_{50}=0.85\mu\text{M}$) and efsevin ($B_{max}=220\%$, $EC_{50}=4.4\mu\text{M}$).

5 Discussion

5.1 Summary

My work aimed at examining the ability of forty different efsevin derivatives for an improved mitochondrial Ca^{2+} uptake, thereby testing their potential as suppressors of cardiac arrhythmogenesis. To this end, three different approaches (*in silico*, *in vitro* and *in vivo*) were performed. Results from the *in silico* screening indicate that none of these forty chemically modified derivatives revealed a superiority of any tested chemical modification. However, in the *in vivo* and *in vitro* screening approaches, three compounds showed an enhancement of mitochondrial Ca^{2+} uptake (P105B10, P105D03 and P105E04). By expanding and adapting the applied methods, I here provide promising opportunities for the discovery of decisive factors in the optimization of MiCUps.

5.2 Limitations of applied screening methods and potential follow-up studies

Since the effect of Ca^{2+} overload in mitochondria is associated with a number of side effects leading to several pathologies, such as heart failure and cardiac cell death⁷⁶, I aimed towards a logical sequence and selection of my screening methods. Initially, I selected a safe and non-invasive method to perform a first screening using computational docking simulations. Computational docking presented an attractive entry point as it represents a comprehensive *in silico* method performed in a rapid, efficient and cost-effective manner^{77,78}. One drawback and key limitation of molecular docking is an adverse and limited selection of possible configurations and imprecise predictors of total binding energies⁷⁹. In this study, a previously identified binding pocket from efsevin² was used as the site for docking of derivatives and all chemical modifications are based on the original efsevin structure providing a comparable pattern. The derivatives were docked in flexible form and the side chains facing the binding site of zVDAC2 were kept flexible, increasing the docking efficiency as well. To take into account the above-mentioned drawbacks, and in order to increase result sensitivity, a follow-up study could address further docking simulations to increase the number of simulations and to optimize the analysis. Lastly, the usage of an additional docking program such as GOLD^{80,81} to broaden data sets could be beneficial. Further exploration of chemical similarities and differences could be obtained by applying principal components analysis (PCA) enabling advanced interpretation of the generated data⁸². Moreover, to analyze bonding behavior, interaction and formation of hydrogen bonds between derivatives and VDAC could be obtained using the program *LigPlot*⁺⁸³. We recently used this program successfully for the identification of the efsevin binding pocket². Generating a more detailed overview of chemical interactions between VDAC2 and derivatives *in silico* could give new insights into potential chemical optimization which then needs to be validated *in vivo* and *in vitro*. While molecular docking may not provide the most accurate method for detecting

protein-ligand interactions on a molecular level, it represents a reliable method for initial selection of potential ligands, which then could be experimentally complemented.

The second screening method I applied was an *in vivo* approach, using a zebrafish model. In particular, the *tremblor* zebrafish model provides a cardiac-specific model for testing the potency of antiarrhythmic drugs. This model enabled me to perform an *in vivo* screening as early as possible in the evaluation process. It represents a straightforward, inexpensive and non-invasive approach. Another advantage of this zebrafish procedure is that it remains outside the scope of animal testing according to the EU Directive (2010/63/EU)⁸⁴ as long as it is confined to less than 5 days after fertilization. Additionally, zebrafish share physiological features with humans, as several other potential drugs and their effects were first identified in zebrafish screening and could then be translated to rodent models as well as humans⁸⁵. Further, as for cardiovascular diseases in humans, 82% of disease-related genes registered in the online database Mendelian inheritance in man (OMIM) share at least one zebrafish ortholog⁸⁶. Moreover, through constant exposure of the embryos with additional dechorionization, an uptake of the substances into the organism is highly probable. Nevertheless, to complement experiments, more detailed information about the derivatives' cell permeability could be addressed using this model. Therefore, other forms of drug application such as microinjection at the embryonic stage could be considered⁸⁷.

As a final method, I chose HL-1 cardiomyocytes, providing a unique opportunity for the quantification of SR-mitochondria Ca^{2+} transfer. This method provides more detailed insights into pharmacodynamics of the tested derivatives⁶⁸. A major advantage is that HL-1 cells show high similarity to primary cardiomyocytes. Further, gene analyses of HL-1 cells demonstrated a similar expression pattern when compared to adult atrial myocytes⁸⁸. To date, there is no comparable cell line which can be kept in culture without losing its adult cardiac phenotype⁸⁹. To point out possible drawbacks of this applied method, potential false-positive effects on SR-mitochondria Ca^{2+} release after intense HL-1 cell treatment applying staining and permeabilization procedures should be controlled for. Follow-up studies could include investigations of cytosolic Ca^{2+} levels in intact HL-1 cells confirming no significant change in Ca^{2+} release⁹⁰.

5.3 Further possible studies on MiCUp candidates

P105D03 performed best among all tested compounds. Nonetheless, no clear improvement with respect to the reference substance efsevin can be observed using the here described methods.

For further exploration on heartbeat restoration in the embryonic zebrafish by derivatives such as P105D03, we could consider cardiac imaging by video line-scan analysis (see *Figure 9*)¹. Using this method, direct comparison to zebrafish treated with efsevin could give an additional insight into derivatives' efficiency focusing on qualitative impact factors such as modulation of heart rate, heart beat rhythm, heart contractility and cardiac remodeling processes. Additionally, expansion of experiments into other model

organisms investigating the anti-arrhythmic effect of derivatives could be considered. For example, the murine model for RyR2-mediated catecholaminergic polymorphic ventricular tachycardia (CPVT)⁶⁸ that generates diastolic intracellular Ca^{2+} waves resulting in an imbalance of Ca^{2+} homeostasis and cardiac arrhythmia could provide additional insights. This approach was previously applied to evaluate efsevin's potency in decreasing arrhythmogenic Ca^{2+} waves and therefore demonstrating anti-arrhythmic effects which were then further explored in human embryonic stem cell-derived cardiomyocytes¹.

Another interesting aim for extending research on derivatives would be to explore their stability and therefore gain additional insights into their pharmacokinetics. Chemical stability represents a direct impact on substances' effectiveness and demonstrates one of the key limitations of efsevin resulting in an immediate limitation for clinical application. Data from derivatives could provide new indications about chemical superiorities focusing on the chemical configurations. Previous work from our lab already explored efsevin's hydrolyzation in human liver microsomes², which could also be applied to the derivatives. Direct correlation of chemical structures should be examined, when comparing their individual duration of complete hydrolyzation.

As cardiac arrhythmia is commonly accompanied with heart failure⁴³, derivatives' potency could also be addressed in a heart failure model. Our lab previously demonstrated increased contractile force of efsevin within a VDAC2-specific heart failure model⁹¹ in mice. Evaluating the contractile force of for example P105D03 in this model would possibly broaden its operational area, as the therapy of heart failure also represents one of the major issues of our time.

5.4 Probable causes and evaluation of obtained outcomes

Conclusively, no significant superior chemical modification based on the efsevin structure was demonstrated by my study. Considerations for this reason suggesting causes for missing improvement in tested derivatives should include the following:

As above-mentioned, stability of the compounds presents a key role in their mode of function and therefore potency as MiCUp. Drug's efficacy is affected by poor stability and could possibly explain obtained results of no significant increase when compared to efsevin. Another possible cause of no clear superiority could directly refer to the chemical modification. Within the modification, several factors may affect its effectiveness. Firstly, the site of modification, secondly, the functional groups utilized for modification and also the synthetization process itself may already have an impact on its efficacy in terms of solubility or storage. For the first two problems, preliminary docking simulations using varying positions of pyrroles and functional groups, could be performed as artificial guide following synthetization of derivatives when possible.

Not only target protein VDAC2, but also its ligand plays an essential role in the mode of action as MiCUp. The recently discovered binding pocket of efsevin exhibits unique and

specific form and features. Therefore, another possible reason for the inefficiency of the derivatives might lie in the fact that the binding pocket cannot be optimized for the derivatives because efsevin exhibits an already optimal binding.

6 Abbreviations

Å	angstrom
BAPTA	1,2-bis(o-aminophenoxy)ethane-N,N,N',N'-tetraacetic acid
Br	bromine
$[Ca^{2+}]_i$	intracellular free Ca^{2+} concentration
$[Ca^{2+}]_m$	intra-mitochondrial Ca^{2+} concentration
°C	centigrade
ATP	Adenosine triphosphate
C	carbon
Ca^{2+}	calcium
$CaCl_2$	calcium chloride
CICR	calcium-induced calcium release
Cl	chloride
cmlc	cardiac myosine light chain
CO_2	carbon dioxide
CPVT	catecholaminergic polymorphic ventricular tachycardia
CRU	calcium releasing unit
CVD	cardiovascular disease
DHPR	dihydropyridine-receptor
ECC	excitation-contraction coupling
EDTA	ethylenediaminetetraacetic acid
EM cells	embryonic stem cells
F	fluorine
GFP	green fluorescent protein
HEPES	4-(2-hydroxyethyl)-1-piperazineethanesulfonic acid
hpf	hours post fertilization
hrs	hours
H_2O	water
ipSC	induced pluripotent stem cell
IMM	inner mitochondrial membrane
K-Asp	L-Aspartic acid potassium salt
kcal	kilocalories
KCl	potassium chloride
kDA	kilodalton
KH_2PO_4	monopotassium phosphate
KO	knock out
LTCC	L-type calcium channel
M	molar
MCU	mitochondrial calcium uniporter

Mg	magnesium
Mg-ATP	magnesium adenosine triphosphate
MgCl ₂	magnesium chloride
MgSO ₄	magnesium sulfate
MiCU _p	mitochondrial Calcium uptake enhancer
min	minute
ml	mililiter
mm	milimeter
mM	milimolar
mol	mole
NaCl	sodium chloride
NaOH	caustic soda
NCX	Na ⁺ / Ca ²⁺ exchanger
nm	nano meter
OMM	outer mitochondrial membrane
p	probability
pH	potential of hydrogen
pdb	protein data bank
PBS	phosphate-buffered saline
RuR	Ruthenium Red
RyR	ryanodine receptors
SCD	sudden cardiac death
SEM	standard error of the mean
SERCA	sarcoplasmic/endoplasmatic reticulum calcium- ATPase
SR	sarcoplasmatic reticulum
TEM	transmission electronic microscope
VDAC	voltage dependent anion channel
μg	microgram
μl	microliter
μM	micromolar

7 List of Figures

Figure 1: Schematic of Ca ²⁺ signaling proteins and excitation-contraction coupling (ECC)	4
Figure 2: Schematic of Ca ²⁺ signaling during systole and diastole	4
Figure 3: Schematic of intracellular Ca ²⁺ release by leaky RyR resulting in cardiac arrhythmia	5
Figure 4: Schematic of cardiac mitochondrial Ca ²⁺ transport represented by VDAC2 and MCU	8
Figure 5: Predicted binding site of efsevin on zVDAC2 obtained in molecular docking ²	10
Figure 6: 2D-schematic of efsevin structure	12
Figure 7: 2D-schematic of efsevin derivatives	13
Figure 8: Docking process: efsevin and VDAC2 as ligands	14
Figure 9: <i>In vivo</i> approach to measure efsevin's effect on heart arrhythmia	16
Figure 10: Schematic of HL-1 assay	20
Figure 11: Efsevin showed highest binding affinity in computational docking screening	21
Figure 12: 20µM efsevin lead to highest rescue of rhythmic cardiac contractions in <i>tremblor</i> zebrafish embryos	23
Figure 13: P105D03 significantly increases rescue of rhythmic cardiac contractions in <i>tremblor</i> zebrafish embryos	24
Figure 14: Dose-dependent mitochondrial Ca ²⁺ uptake (in %) by efsevin in HL-1 cardiomyocytes	25
Figure 15: SR-mitochondria Ca ²⁺ transfer in HL1-cardiomyocytes	26
Figure 16: Statistical analysis of SR-mitochondria Ca ²⁺ transfer in HL-1 cardiomyocytes	26
Figure 17: Derivative P105B10 displayed most efficient mitochondrial Ca ²⁺ uptake in HL-1 cardiomyocytes	27
Table 1: Derivatives display no clear correlations between the location and type of the chemical modifications and binding affinities obtained in computational screening	22
Table 2: Derivatives show no chemical similarity according to their potency of cardiac rhythmicity rescue in <i>tremblor</i> zebrafish	24

8 References

1. Shimizu, H. *et al.* Mitochondrial Ca^{2+} uptake by the voltage-dependent anion channel 2 regulates cardiac rhythmicity. *Elife* (2015). doi:10.7554/eLife.04801
2. Wilting, F. *et al.* The antiarrhythmic compound efsevin directly modulates voltage-dependent anion channel 2 by binding to its inner wall and enhancing mitochondrial Ca^{2+} uptake. *Br. J. Pharmacol.* bph.15022 (2020). doi:10.1111/bph.15022
3. Virani, S. S. *et al.* Heart Disease and Stroke Statistics—2021 Update. *Circulation* **143**, (2021).
4. Leal, J., Luengo-Fernández, R., Gray, A., Petersen, S. & Rayner, M. Economic burden of cardiovascular diseases in the enlarged European Union. *Eur. Heart J.* **27**, 1610–1619 (2006).
5. WHO. The top 10 causes of death. <https://www.who.int/news-room/fact-sheets/detail/> (2020).
6. WHO. WHO reveals leading causes of death and disability worldwide: 2000-2019. <https://www.who.int/news/item/09-12-2020-who-reveals-leading-causes-of-death-and-disability-worldwide-2000-2019>. Available at: <https://www.who.int/news/item/09-12-2020-who-reveals-leading-causes-of-death-and-disability-worldwide-2000-2019>.
7. WHO. Cardiovascular diseases (CVDs). <https://www.who.int/news-room/fact-sheets/detail/c>
8. Mathers, C. D., Boerma, T., Fat, D. M. & Mathers, C. Global and regional causes of death. *Br. Med. Bull.* **92**, 7–32 (2009).
9. Mehra, R. Global public health problem of sudden cardiac death. *J. Electrocardiol.* **40**, S118–S122 (2007).
10. Srinivasan, N. T. & Schilling, R. J. Sudden Cardiac Death and Arrhythmias. *Arrhythmia Electrophysiol. Rev.* **7**, 111–117 (2018).
11. Tang, D. H., Gilligan, A. M. & Romero, K. Economic Burden and Disparities in Healthcare Resource Use Among Adult Patients with Cardiac Arrhythmia. (2013). doi:10.1007/s40258-013-0070-9
12. Pape, H. C., Kurtz, A. & Silbernagl, S. *Physiologie*. (Thieme Verlag, 2014).
13. Silverman, M. E. & Hollman, A. Discovery of the sinus node by Keith and Flack: on the centennial of their 1907 publication. *Heart* **93**, 1184 (2007).
14. Engelmann, T. W. Ueber die Leitung der Erregung im Herzmuskel. *Arch. für die Gesamte Physiol. des Menschen und der Thiere* **11**, 465–480 (1875).
15. Rohr, S. Role of gap junctions in the propagation of the cardiac action potential. *Cardiovasc. Res.* **62**, 309–322 (2004).
16. Bers, D. M. Cardiac excitation–contraction coupling. *Nature* **415**, 198–205 (2002).
17. Fabiato, A. & Fabiato, F. CALCIUM-INDUCED RELEASE OF CALCIUM FROM THE SARCOPLASMIC RETICULUM OF SKINNED CELLS FROM ADULT HUMAN, DOG, CAT, RABBIT, RAT, AND FROG HEARTS AND FROM FETAL AND NEW-BORN RAT VENTRICLES. *Ann. N. Y. Acad. Sci.* **307**, 491–522 (1978).

18. Endo, M., Tanaka, M. & Ogawa, Y. Calcium Induced release of calcium from the Sarcoplasmic Reticulum of Skinned Skeletal Muscle Fibres. *Nature* (1970). doi:10.1038/228034a0
19. Bers, D. M. *Excitation-Contraction Coupling and Cardiac Contractile Force*. **122**, (Springer Netherlands, 1993).
20. Bassani, R. A., Bassani, J. W. & Bers, D. M. Mitochondrial and sarcolemmal Ca²⁺ transport reduce [Ca²⁺]_i during caffeine contractures in rabbit cardiac myocytes. *J. Physiol.* **453**, 591–608 (1992).
21. BioRender. (2021). Available at: <https://biorender.com/>. (Accessed: 24th November 2021)
22. Karow, T. & Lang-Roth, R. *Allgemeine und spezielle Pharmakologie und Toxikologie*. (2018).
23. Landstrom, A. P., Dobrev, D. & Wehrens, X. H. T. Calcium Signaling and Cardiac Arrhythmias. *Circ. Res.* **120**, 1969–1993 (2017).
24. King, G. S. & Hashmi, M. F. King GS, Hashmi MF. *Antiarrhythmic Medications*. [Updated 2019 Oct 24]. In: *StatPearls [Internet]*. Treasure Island (FL): StatPearls Publishing; 2020 Jan-. Available from: <https://www.ncbi.nlm.nih.gov/books/NBK482322/>. In: *StatPearls [Internet]*. Treasure Island (FL): StatPearls Publishing (StatPearls Publishing).
25. Harrison, D. C. A rational scientific basis for subclassification of antiarrhythmic drugs. *Trans. Am. Clin. Climatol. Assoc.* **97**, 43–52 (1986).
26. Lei, M., Wu, L., Terrar, D. A. & Huang, C. L.-H. Modernized Classification of Cardiac Antiarrhythmic Drugs. *Circulation* **138**, 1879–1896 (2018).
27. Nattel, S. *Experimental evidence for proarrhythmic mechanisms of antiarrhythmic drugs*. *Cardiovascular Research* **37**, (1998).
28. Zipes, D. P. Proarrhythmic effects of antiarrhythmic drugs. *Am. J. Cardiol.* **59**, 26E-31E (1987).
29. Greene, H. L., Roden, D. M., Katz, R. J. & Raymond, F. ; *The Cardiac Arrhythmia Suppression Trial : First CAST. .. Then CAST-1*.
30. Dusman, R. E. *et al. Clinical Features of Amiodarone-Induced Pulmonary Toxicity*.
31. Kennedy, H. L. *et al.* Beta-blocker therapy in the Cardiac Arrhythmia Suppression Trial. CAST Investigators. *Am. J. Cardiol.* **74**, 674–80 (1994).
32. Santangeli, P., Di Biase, L. & Natale, A. Ablation versus drugs: what is the best first-line therapy for paroxysmal atrial fibrillation? Antiarrhythmic drugs are outmoded and catheter ablation should be the first-line option for all patients with paroxysmal atrial fibrillation: pro. *Circ. Arrhythm. Electrophysiol.* **7**, 739–46 (2014).
33. Shiferaw, Y., Aistrup, G. L. & Wasserstrom, J. A. Intracellular Ca²⁺ waves, afterdepolarizations, and triggered arrhythmias. *Cardiovasc. Res.* **95**, 265–8 (2012).
34. Njegic, A., Wilson, C. & Cartwright, E. J. Targeting Ca²⁺ Handling Proteins for the Treatment of Heart Failure and Arrhythmias. *Front. Physiol.* **11**, 1068 (2020).

35. Behrends, J. C., Kurtz, A. & et al. *Physiologie*. (Thieme Verlag, 2010).
36. Roe, A. T., Frisk, M. & Louch, W. E. Targeting cardiomyocyte Ca²⁺ homeostasis in heart failure. *Curr. Pharm. Des.* **21**, 431–48 (2015).
37. Coppini, R., Ferrantini, C., Mugelli, A., Poggesi, C. & Cerbai, E. Altered Ca²⁺ and Na⁺ Homeostasis in Human Hypertrophic Cardiomyopathy: Implications for Arrhythmogenesis. *Front. Physiol.* **9**, 1391 (2018).
38. Bolland, M. J. *et al.* Effect of calcium supplements on risk of myocardial infarction and cardiovascular events: meta-analysis. *BMJ* **341**, c3691 (2010).
39. Yano, M., Ikeda, Y. & Matsuzaki, M. Altered intracellular Ca²⁺ handling in heart failure. *J. Clin. Invest.* **115**, 556–64 (2005).
40. Hasenfuss, G. *et al.* Calcium handling proteins in the failing human heart. *Basic Res. Cardiol.* **92**, 87–93 (1997).
41. O'Rourke, B. *et al.* Mechanisms of Altered Excitation-Contraction Coupling in Canine Tachycardia-Induced Heart Failure, I. *Circ. Res.* **84**, 562–570 (1999).
42. Wehrens, X. H. T. & Marks, A. R. Novel therapeutic approaches for heart failure by normalizing calcium cycling. *Nat. Rev. Drug Discov.* **3**, 565–574 (2004).
43. Chakko, S., De Marchena, E., Kessler, K. M. & Myerburg, R. J. Ventricular arrhythmias in congestive heart failure. *Clin. Cardiol.* **12**, 525–530 (1989).
44. Priori, S. G. *et al.* Mutations in the Cardiac Ryanodine Receptor Gene (*hRyR2*) Underlie Catecholaminergic Polymorphic Ventricular Tachycardia. *Circulation* **103**, 196–200 (2001).
45. Nattel, S. & Dobrev, D. The multidimensional role of calcium in atrial fibrillation pathophysiology: mechanistic insights and therapeutic opportunities. doi:10.1093/eurheartj/ehs079
46. Pogwizd, S. M., Schlotthauer, K., Li, L., Yuan, W. & Bers, D. M. Arrhythmogenesis and Contractile Dysfunction in Heart Failure. *Circ. Res.* **88**, 1159–1167 (2001).
47. Brown, D. A. & O'rourke, B. Cardiac mitochondria and arrhythmias. doi:10.1093/cvr/cvq231
48. DELUCA, H. F. & ENGSTROM, G. W. Calcium uptake by rat kidney mitochondria. *Proc. Natl. Acad. Sci. U. S. A.* **47**, 1744–50 (1961).
49. Palmer, J. W., Tandler, B. & Hoppel, C. L. Biochemical properties of subsarcolemmal and interfibrillar mitochondria isolated from rat cardiac muscle. *J. Biol. Chem.* (1977).
50. Lukyanenko, V., Chikando, A. & Lederer, W. J. Mitochondria in cardiomyocyte Ca²⁺ signaling. *Int. J. Biochem. Cell Biol.* **41**, 1957–71 (2009).
51. Lüllmann-Rauch, R. *Histologie*. (Thieme Verlag, 2012).
52. Sharma, V. K., Ramesh, V., Franzini-Armstrong, C. & Sheu, S. S. Transport of Ca²⁺ from sarcoplasmic reticulum to mitochondria in rat ventricular myocytes. *J. Bioenerg. Biomembr.* **32**, 97–104 (2000).
53. Boncompagni, S. *et al.* Mitochondria are linked to calcium stores in striated muscle by developmentally regulated tethering structures. *Mol. Biol. Cell* **20**, 1058–67

- (2009).
54. Nguyen, B. Y. *et al.* Mitochondrial function in the heart: the insight into mechanisms and therapeutic potentials. *Br. J. Pharmacol.* **176**, 4302–4318 (2019).
 55. Gincel, D., Zaid, H. & Shoshan-Barmatz, V. *Calcium binding and translocation by the voltage-dependent anion channel: a possible regulatory mechanism in mitochondrial function.* *Biochem. J* **358**, (2001).
 56. Kirichok, Y., Krapivinsky, G. & Clapham, D. E. The mitochondrial calcium uniporter is a highly selective ion channel. *Nature* **427**, 360–364 (2004).
 57. Patron, M. *et al.* MICU1 and MICU2 finely tune the mitochondrial Ca²⁺ uniporter by exerting opposite effects on MCU activity. *Mol. Cell* **53**, 726–37 (2014).
 58. Wang, Y. *et al.* Structural Mechanism of EMRE-Dependent Gating of the Human Mitochondrial Calcium Uniporter. *Cell* **177**, 1252-1261.e13 (2019).
 59. Schein, S. J., Colombini, M. & Finkelstein, A. Reconstitution in planar lipid bilayers of a voltage-dependent anion-selective channel obtained from paramecium mitochondria. *J. Membr. Biol.* (1976). doi:10.1007/BF01869662
 60. Colombini, M. Voltage gating in the mitochondrial channel, VDAC. *J. Membr. Biol.* **111**, 103–111 (1989).
 61. Naghdi, S. & Hajnóczky, G. VDAC2-specific cellular functions and the underlying structure. *Biochim. Biophys. Acta* **1863**, 2503–14 (2016).
 62. Dolder, M. *et al.* Crystallization of the human, mitochondrial voltage-dependent anion-selective channel in the presence of phospholipids. *J. Struct. Biol.* (1999). doi:10.1006/jsbi.1999.4141
 63. Schredelseker, J. *et al.* High Resolution Structure and Double Electron-Electron Resonance of the Zebrafish Voltage-dependent Anion Channel 2 Reveal an Oligomeric Population. *J. Biol. Chem.* **289**, 12566–12577 (2014).
 64. Hiller, S. *et al.* Solution structure of the integral human membrane protein VDAC-1 in detergent micelles. *Science* **321**, 1206–10 (2008).
 65. Bayrhuber, M. *et al.* Structure of the human voltage-dependent anion channel. *Proc. Natl. Acad. Sci.* **105**, 15370–15375 (2008).
 66. Subedi, K. P. *et al.* Voltage-dependent anion channel 2 modulates resting Ca²⁺ sparks, but not action potential-induced Ca²⁺ signaling in cardiac myocytes. *Cell Calcium* **49**, 136–143 (2011).
 67. Langenbacher, A. D. *et al.* Mutation in sodium-calcium exchanger 1 (NCX1) causes cardiac fibrillation in zebrafish. *Proc. Natl. Acad. Sci. U. S. A.* (2005). doi:10.1073/pnas.0502679102
 68. Schweitzer, M. K. *et al.* Suppression of Arrhythmia by Enhancing Mitochondrial Ca²⁺ Uptake in Catecholaminergic Ventricular Tachycardia Models. *JACC Basic to Transl. Sci.* **2**, (2017).
 69. Trott, O. & Olson, A. J. AutoDock Vina: Improving the speed and accuracy of docking with a new scoring function, efficient optimization, and multithreading. *J. Comput. Chem.* NA-NA (2009). doi:10.1002/jcc.21334
 70. Claycomb, W. C. *et al.* HL-1 cells: a cardiac muscle cell line that contracts and retains phenotypic characteristics of the adult cardiomyocyte. *Proc. Natl. Acad.*

- Sci. U. S. A.* **95**, 2979–84 (1998).
71. Marvin | ChemAxon. Available at: <https://chemaxon.com/products/marvin>. (Accessed: 26th October 2020)
 72. Morris, G. M. *et al.* AutoDock4 and AutoDockTools4: Automated Docking with Selective Receptor Flexibility. *J. Comput. Chem.* **30**, 2785 (2009).
 73. Westerfield, M. *The Zebrafish Book*. Eugene (2000).
 74. Nguyen, C. T., Lu, Q., Wang, Y. & Chen, J.-N. Zebrafish as a model for cardiovascular development and disease. *Drug Discov. Today. Dis. Models* **5**, 135 (2008).
 75. WEBMAXC STANDARD. Available at: <https://web.stanford.edu/~cpatton/webmaxcS.htm>. (Accessed: 15th November 2018)
 76. Giorgi, C., Marchi, S. & Pinton, P. The machineries, regulation and cellular functions of mitochondrial calcium. *Nat. Rev. Mol. Cell Biol.* **19**, 713–730 (2018).
 77. Macalino, S. J. Y., Gosu, V., Hong, S. & Choi, S. Role of computer-aided drug design in modern drug discovery. *Arch. Pharm. Res.* **38**, 1686–1701 (2015).
 78. Meng, X.-Y., Zhang, H.-X., Mezei, M. & Cui, M. Molecular docking: a powerful approach for structure-based drug discovery. *Curr. Comput. Aided. Drug Des.* **7**, 146–57 (2011).
 79. Bender, B. J. *et al.* A practical guide to large-scale docking. *Nat. Protoc.* **16**, 4799–4832 (2021).
 80. Liebeschuetz, J. W., Cole, J. C. & Korb, O. Pose prediction and virtual screening performance of GOLD scoring functions in a standardized test. *J. Comput. Aided. Mol. Des.* **26**, 737–748 (2012).
 81. Pagadala, N. S., Syed, K. & Tuszynski, J. Software for molecular docking: a review. *Biophys. Rev.* **9**, 91–102 (2017).
 82. Giuliani, A. The application of principal component analysis to drug discovery and biomedical data. *Drug Discov. Today* **22**, 1069–1076 (2017).
 83. Laskowski, R. A. & Swindells, M. B. LigPlot+: multiple ligand-protein interaction diagrams for drug discovery. *J. Chem. Inf. Model.* **51**, 2778–86 (2011).
 84. *DIRECTIVE 2010/63/EU OF THE EUROPEAN PARLIAMENT AND OF THE COUNCIL of 22 September 2010 on the protection of animals used for scientific purposes (Text with EEA relevance).*
 85. Asnani, A. & Peterson, R. T. The zebrafish as a tool to identify novel therapies for human cardiovascular disease. *Dis. Model. Mech.* **7**, 763–7 (2014).
 86. Howe, K. *et al.* The zebrafish reference genome sequence and its relationship to the human genome. *Nature* **496**, 498–503 (2013).
 87. Schubert, S., Keddig, N., Hanel, R. & Kammann, U. Microinjection into zebrafish embryos (*Danio rerio*) - a useful tool in aquatic toxicity testing? *Environ. Sci. Eur.* **26**, 32 (2014).
 88. Claycomb, W. C. *et al.* HL-1 cells: a cardiac muscle cell line that contracts and retains phenotypic characteristics of the adult cardiomyocyte. *Proc. Natl. Acad.*




Sci. U. S. A. **95**, 2979–84 (1998).

89. White, S. M., Constantin, P. E. & Claycomb, W. C. Cardiac physiology at the cellular level: use of cultured HL-1 cardiomyocytes for studies of cardiac muscle cell structure and function. *Am. J. Physiol. Circ. Physiol.* **286**, H823–H829 (2004).
90. Sander, P. *et al.* Approved drugs ezetimibe and disulfiram enhance mitochondrial Ca²⁺ uptake and suppress cardiac arrhythmogenesis. *Br. J. Pharmacol.* **178**, 4518–4532 (2021).
91. Shankar, T. S. *et al.* Cardiac-specific deletion of voltage dependent anion channel 2 leads to dilated cardiomyopathy by altering calcium homeostasis. *Nat. Commun.* **12**, 4583 (2021).

9 Acknowledgement

I would like to thank Paulina Sander and Fabiola Wilting for their great support during my work and Brigitte Mayerhofer for technical assistance. Also, I would like to thank Alexandra Klein for her constant support with my work. This work was supported by „Molekulare und klinisch-translazionale Medizin“- program provided by Ludwig-Maximilians-Universität Munich and by Professor Ohyun Kwon providing me with the forty efsevin derivatives. Also, my thanks go to my MD supervisors Thomas Gudermann and Johann Schredelseker.

10 Affidavit

	LUDWIG- MAXIMILIANS- UNIVERSITÄT MÜNCHEN	Promotionsbüro Medizinische Fakultät		
Eidesstattliche Versicherung				

Schedel, Anna Sophia

Name, Vorname

Ich erkläre hiermit an Eides statt, dass ich die vorliegende Dissertation mit dem Titel:

Optimization of a mitochondrial calcium uptake enhancer for the treatment of cardiac arrhythmia

selbständig verfasst, mich außer der angegebenen keiner weiteren Hilfsmittel bedient und alle Erkenntnisse, die aus dem Schrifttum ganz oder annähernd übernommen sind, als solche kenntlich gemacht und nach ihrer Herkunft unter Bezeichnung der Fundstelle einzeln nachgewiesen habe.

Ich erkläre des Weiteren, dass die hier vorgelegte Dissertation nicht in gleicher oder in ähnlicher Form bei einer anderen Stelle zur Erlangung eines akademischen Grades eingereicht wurde.

Sankt Gallen, 02.01.2024

Ort, Datum

_____ Anna Sophia Schedel _____

Unterschrift Doktorandin bzw. Doktorand